Abstracts of the Papers Published in Other Journals by the Staff members of the Institute from July, 1968 to June, 1969

Abstracts of the Papers Published in Other Journals by the Staff members of the Institute from July, 1968 to June, 1969

Nuclear Chemistry

Breakup of Deuteron by Impact of Alpha Particle and Deuteron. Tetsumi Tanabe. *J. Phys. Soc. Japan,* **25,** 21 (1968).—The $D(\alpha, p\alpha)n$ and $D(d, pd)n$ reactions were studied by using 29.2 MeV alpha particles and 14.6 MeV deuterons respectively. Coincidence energy spectra of two charged particles emitted from each reaction were measured at coplaner and non-coplaner angles. The energy spectra of the $D(\alpha, p\alpha)n$ reaction indicate the effect of the resonance between nucleons and alpha particles corresponding to the He^5 and Li^5 ground state and show at some angles broad peaks for spectator neutrons with zero energy. The energy spectrum of the $D(d, pd)n$ reaction shows only one broad peak for spectator neutrons. The impulse approximation calculations represent fairly well both the energy spectra and the angular dependence. It is concluded that the deuteron breakup mechanism is to occur through the quasi-free scattering of an incident particle from a nucleon in the deuteron.

***j*-Forbidden (d, p) Stripping Reactions on C^{12}, O^{16} and Mg^{24}.** Kazuhiko Hosono. *J. Phys. Soc. Japan,* **25,** 36 (1968).—High resolution studies of the (d, p) reaction on C^{12} at 14.6 MeV, O^{16} at 14.3 MeV and Mg^{24} at 12.3 MeV were performed. The C^{12} (d, p) C^{13} reaction leading to the ground and the 3.68 MeV states was also investigated from 14.7 MeV down to 12.3 MeV. Some transitions which cannot be explained by simple stripping process were observed. Most of angular distributions of protons from the *j*-forbidden stripping reaction showed a structureless pattern and the cross section was 10-30% of that of simple stripping process. Simple PWBA analyses based on the two step process and on the knock out process were made and a possibility of the two step process was suggested. The structure of some excited states was discussed in connection with the reaction mechanism.

Instrumentations of the 1 GeV Proton-Nucleus Reaction Experiment. Noboru Fujiwara. *Genshikaku-Kenkyu,* **13,** 234 (1968), in Japanese.—Recent experiments in the Brookhaven National Laboratory, U. S. A., done by using the 1 GeV proton beam from the Cosmotron are reviewed. High energy nuclear physics need some skill different from those of low energy nuclear physics because of the ambiguity in the kinematics and 0.1% energy resolution is necessary to detect the elastic scattering from nuclei. Wire spark chambers and on-line data processing fascillities used in these experiments are critically introduced. Some experimental results show that multiple scattering of protons inside the target nucleus is obvious and the nucleon correlation in the nucleus plays an important role.

Inelastic Alpha-Particle Scattering on Copper 65 at 29 MeV. I. Kumabe, M. Matoba and E. Takasaki. *J. Phys. Soc. Japan,* **25,** 301 (1968).—The excited states of ^{65}Cu have been studied by inelastic scattering of 29 MeV alpha particles. The over-all energy resolution of about 70 KeV in this experiment enabled to resolve six quadrupole and eight octupole states. Transition strengths were extracted for these states using the DWBA method. The results were compared with the weak-coupling core-excitation model and with the theoretical calculation of Thankappan and True.

(α, t) Reaction on Medium-Weight Odd-Mass Nuclei (1). ^{51}V and ^{55}Mn. Masaru Matoba. *Nuclear Phys.*, **A118,** 207 (1968).—The (α, t) reactions on ^{51}V and ^{55}Mn have been studied at an incident alpha energy of 29.0 MeV using an *E-ΔE* semiconductor detector telescope. Angular distributions were obtained and analysed by the DWBA theory. Zero-range DWBA calculations without radial cut-offs gave a reasonable fit to the data with depths of the real parts of the alpha and triton potentials of 183.7 and 149.0 MeV, respectively. The *l*-values and spectroscopic factors were deduced from the transitions leading to 15 low-lying states of ^{52}Cr and ^{56}Fe. The results were compared with the seniority scheme and the sum rule of the *j-j* coupling shell model and gave information about the $(1f_{7/2})^n$ proton states in ^{52}Cr and ^{56}Fe.

B^{11} (α, Li^7) Be^8 Reaction at 28.4 and 29.0 Mev. S. Kakigi, N. Fujiwara, K. Fukunaga, D. C. Nguyen, S. Yamashita and T. Yanabu. *J. Phys. Soc. Japan,* **25,** 1214 (1968).—Li^7 ions from the B^{11} (α, Li^7) Be^8 reaction were detected with a 50 μ thick SSD covered with aluminum absorbers. The analyses suggest that the compound nucleus process is not favorable to the B^{11} (α, Li^7) Be^8 (g.s.) reaction. The angular distributions of Li^7 (0.478 MeV state) can be reproduced by the calculation based on the triton pickup process. The feature of the angular distributions of Li^7 (g.s.) is quite different from that of Li^7 (0.478 MeV state) and is qualitatively explained by the triton pickup process and the Li^7 knockout process interfering with each other.

$Li^7+\alpha \rightarrow t+\alpha+\alpha$ Reaction. Seishi Matsuki. *Soryushiron-Kenkyu,* **39,** 303 (1969), in Japanese.—Tritons from the reaction $Li^7+\alpha \rightarrow t+\alpha+\alpha$ were detected. The energy spectra of tritons show sharp peaks corresponding to the 0^+ and 2^+ state of Be^8. Further, a broad peak was observed at the Be^8 excitation energy of 7 MeV. These peaks were compared with the predictions of the density of state function theory. The broad peak at 7 MeV of Be^8 is of asymmetric shape and it was suggested that this peak represents the decay tritons from the excited state of Li^7.

Three-Body Reaction of Light Nuclei. Noboru Fujiwara. *Soryushiron-Kenkyu,* **39,** 305 (1969), in Japanese.—The characteristics of final three body nuclear reactions are introduced. Two of the final three bodies can be in various states including resonances because of the momentum distribution of the rest particle. $B^{11}+\alpha \rightarrow \alpha+\alpha+Li^7$ reaction and $B^{11}+p \rightarrow \alpha+\alpha+\alpha$ reaction are especially reviewed from the standpoint of the overlapping of two-body resonances. The resonance width of two alpha particle system is clearly affected by the presence of the remaining particle. Therefore, three particles spend their times in a common interaction volume. The posibility is discussed to investigate the nuclear structure from outside the nucleus by the use of three-body reaction.

Quasi-Free Scattering in the Reaction Be^9 (p, pα) He^5 at 55 MeV. S. Yamashita, S. Kakigi, N. Fujiwara, D. C. Nguyen, K. Hosono, S. Matsuki, T. Tanabe, T. Yanabu, K. Takimoto, K. Ogino and R. Ishiwari. *J. Phys. Soc. Japan,* **26.** 1078 (1969).—The reaction Be^9 (p, pα) He^5 (g'nd) was studied by coincidence measurements of emitted protons and alpha-particles. The angular correlation distributions were obtained in three manners. All of the distributions had a maximum at a pair of angles which corresponds kinematically to the zero momentum of the recoil nucleus. The yields at the recoilless angles were almost proportional to the differential cross section of the free proton-helium elastic scattering at the corresponding angle. The absolute cross section and the width of the peak appearing in the angular correlation distribution were in fairly good agreement with the results given previously by the experiment on the reaction Be^9 (α, 2α) He^5 (g'nd) at 28 MeV.

Excitation Functions for the (d, p) Reactions on ^{96}Ru, ^{102}Ru and ^{104}Ru. A. Mito, K. Komura, T. Mitsugashira and K. Otozai. *Nuclear Phys.*, **A129,** 165 (1969). —Excitation functions for (d, p) reactions on ^{96}Ru, ^{102}Ru and ^{104}Ru were measured with the activation method up to 14.0 MeV deuteron energy. The results were explained with the modified Peaslee theory by using different values of the absorption parameter ρ. It was found on the doubly even target nuclei that the values of ρ for (d, p) reactions became large as their isotopic numbers N-Z increased.

Elastic and Inelastic Scattering of 14.7 MeV Deuterons and of 29.4 MeV Alpha-Particles by Li^6 and Li^7. S. Matsuki, S. Yamashita, K. Fukunaga, D. C. Nguyen, N. Fujiwara and T. Yanabu. *J. Phys. Soc. Japan,* **26,** 1344 (1969). —The angular distributions of alpha-particles and deuterons scattered elastically and inelastically by Li^6 and Li^7 were measured. The 2.18 MeV state of Li^6, the 0.478 MeV and the 4.63 MeV states of Li^7 were appreciably excited. The experimental angular distributions were analysed with the DWBA theory, and the deformation parameters of the above mentioned states were determined.

Experimental results and the DWBA analysis showed the existence of some difference between the inelastic scattering of alpha-particles by Li^6 and by Li^7, while no appreciable difference was observed in the case of the deuteron scattering. The DWBA calculation predicted larger quadrupole deformations of the excited states of Li^6 and Li^7 as compared with rotational model calculations of the energy levels.

Radiationless Annihilation of Positrons in Lead. S. Shimizu, T. Mukoyama and Y. Nakayama. *Phys. Rev.*, **173,** 405 (1968).—A process of positron annihilation without emission of radiation, *radiationless* or *zero-quantum annihilation,* has been investigated experimentally. A theory for this phenomenon has also been developed. The 300-keV positrons were focused on a thin lead target by the use of a Siegbahn-Slätis intermediate-image spectrometer mounted with Na^{22} as a positron source. The shell electrons ejected from the lead foil were observed with a lithium-drifted silicon detector mounted immediately behind the foil. We have observed a small peak in the expected energy region of the electron spectrum. This has been attributed to the shell electrons ejected from the lead foil. The effect of target thickness has been examined carefully as an important factor influencing our observations. Using the experimental data

obtained, we have attempted to estimate the total cross section of this annihilation process in lead. Our experimental result is $\sigma_{\text{exptl}} = 0.8_{-0.3}{}^{+0.4} \times 10^{-26}$ cm^2 as a sum of those for *K-K*, *K-L*, *K-M*, and *L-L* pairs of shell electrons in a lead atom for 300-KeV positrons. The calculated cross section we obtained is $\sigma_{\text{calc}} = 0.727 \times 10^{-26}$ cm^2. Our experimental value is in agreement with the calculated result within the experimental error. The present work has established the experimental evidence for this mode of positron annihilation, and has furthered understanding of the process.

Single-Quantum Annihilation of Positrons. H. Mazaki, M. Nishi and S. Shimizu. *Phys. Rev.*, **171,** 408 (1968).—Total cross sections for the single-quantum annihilation of positrons in five elements have been measured. The monoenergetic positron beam was obtained by the use of a Siegbahn-Slätis intermediate-image spectrometer mounted with a Na^{22} source. Thin foils of $_{50}$Sn, $_{73}$Ta, $_{79}$Au, $_{82}$Pb, and $_{92}$U were used, successively, as targets mounted at the focal point of the spectrometer. The monoenergetic γ photons due to the single-quantum annihilation were measured in coincidence with accompanying *K* x-rays from the target, using the NaI (Tl) scintillation detectors. The effect of the finite target thickness was evaluated carefully by measuring the energy distribution of incident positrons in the thin target. The exponent of *Z* in the total cross section of this process for the incident positrons with 300-keV kinetic energy has been found to be 4.93 ± 0.31, in agreement with calculations by Johnson *et al.* The energy dependence of the total cross sections, measured for $_{82}$Pb and $_{92}$U in the positron energy range from 250 to 400 keV, has also been found to be in fairly good agreement with theoretical values calculated by other workers using the relativistic Coulomb wave functions for both the *K*-shell electron and the incident positron.

Positon Straggling through Thin Foils. M. Nishi and H. Mazaki. *Nucl. Phys.*, **A119,** 467 (1968).—Experimental study of positon straggling in thin absorbers has been performed with the aid of a Siegbahn-Slätis intermediate-image spectrometer mounted with a ^{22}Na source. The energy of the incident positons is chosen as 300 keV. Targets used are aluminum, nickel, tin, tantalum and lead with thickness up to about 40 mg/cm^2. The most probale energy losses of positons in traversing the absorbers show good agreement with the Rohrlich-Carlson theory when the absorbers are thin enough, but for rather thick absorbers the experimental results fail to fit to the theory. It has also been found that the straggling distributions agree well with the theoretical values calculated from the Blunck-Leisegang theory.

Analytical Chemistry

The Coprecipitation and the spectrophotometric Determination of Uranium as Dibenzoylmethane Chelate. T. Shigematsu, M. Tabushi, M. Matsui and M. Munakata. *Bull. Chem. Soc. Japan*, **41,** 1610 (1968).—The coprecipitation and direct-photometric method was applied to the uranium β-diketonate system; uranyl ion was coprecipitated as dibenzoylmethanate with *O*-phenylphenol and determined spectrophotometrically after the precipitate was dissolved in butyl acetate. The effect of ligand concentration on the per cent coprecipitation-pH curve was studied

and the curve was not affected by the ligand concentration in the range from 2×10^{-2} to 4×10^{-4} M. Over the 200 mg of *O*-phenylphenol, an almost quantitative coprecipitation was obtained, though the absorbance slightly decreased with the increase in the coprecipitant amount (about 2% per 1 g *O*-phenylphenol). As many diverse ions interfered with the determination of uranium, the solution of calcium-EDTA chelate was used as a masking agent. When a small amount of alkylamine was added, the recovery of uranium became more complete. The effect of alkylamine was probably caused by the adduct formation of uranium chelate with alkylamine.

Studies on Adduct Formation of β-Diketone Chelates with Heterocyclic Bases. T. Shigematsu, M. Tabushi, M. Matsui and M. Munakata. *Bull. Chem. Soc. Japan,* **41,** 2656 (1968).—Stability constants of the 1:1-adducts with heterocyclic Lewis bases on copper chelates of six β-diketones and two ethylesters of β-ketoacids (Cu (ligand)$_2$·base) were determined by spectrophotometric measurements in visible region and the effects of β-diketone substituents, Lewis bases and organic solvents on the stability constants were studied. Terminal alkyl groups of β-diketones hardly hindered the adduct formation, because the adducts of β-diketone chelates except acetylacetone chelate had similar stability constants. Solvent effect was due to the formation of the solvates of the chelates or the solvation of N-base with solvent. This is related to the abnormal position of chloroform in the order of the adduct stability compared with oxygen-containing solvents. Infrared spectra indicate that the metal-oxygen bonding, as well as the basicity of Lewis bases is considered as an essential factor in the adduct formation of metal β-diketone chelates.

Fluorometric Determination of Trace Amount of Aluminum in Sea-Water. Y. Nishikawa, K. Hiraki, K. Morishige, A. Tsuchiyama and T. Shigematsu. *Bunseki Kagaku,* **17,** 1092 (1968), in Japanese.—The fluorometric method for the determination of aluminum [This Journal, **16,** 692 (1967)] was adopted for analysis of aluminum in sea water.

Sample water containing 0.003-2 μg of aluminum was treated with 0.5 ml of 0.01% lumogallion solution, and pH was adjusted to 5.0 (CH_3COONH_4-CH_3COOH buffer). It was heated at 80°C for 20 minutes, and the intensity of fluorescence of the solution was measured. Ferric iron interfered with this procedure, and hence the aluminum content in sample water was determined by using a calibration curve obtained in the presence of equivalent amounts of ferric iron.

The amounts of dissolved aluminum and the particle size distribution of aluminum in suspension were determined successfully by the above procedure. The freezing storage of sea water gave good results.

Synergistic Effect in Solvent Extraction —Metal β-diketonate extraction system—T. Honjyo and T. Shigematsu. *Kagaku (Kyoto),* **23,** 708 (1968), in Japanese.—Review.

Fluorometric Analysis. T. Shigematsu and R. Tabata. *Bunseki Kagaku,* **17,** 33R (1968), in Japanese.—Review.

The Extraction-Spectrophotometric Determination of Cobalt (II) with Benzoyltrifluoroacetone—Tri-*n*-octylphosphine Oxide. T. Shigematsu and T.

Honjyo. *Bunseki Kagaku,* **18,** 68 (1969), in Japanese. —The solvent extraction and spectrophotometric determination of cobalt (II) with benzoyltrifluoroacetone (BFA) in the presence of tri-*n*-octylphosphine oxide (TOPO) in cyclohexane were investigated.

The sample solution (pH 5.5-6.0) was shaken with 10^{-3} *M* BFA solution containing 10^{-2} *M* TOPO. The rapid, complete and quantitative extraction of cobalt (II) up to 20 ppm was performed. The composition of the extracted species was estimated to be Co (BFA) $_2$TOPO. In the absence of TOPO, however, only traces of cobalt could be extracted. The amount of cobalt(II) was determined by measuring absorbance of cyclohexane solution at 380 mμ or 390 mμ. Molar extinction coefficients were 3700 (380 mμ) and 2300 (390 mμ). Ni(II), Mn(II), Cu(II), Fe(II), citric acid and EDTA interfered.

The Synergistic Effect in Solvent Extraction. The Effect of Carboxylic Acid on the Solvent Extraction of Europium(III) with Benzoyltrifluoroacetone. T. Shigematsu, M. Tabushi, M. Matsui and T. Honjyo. *Bull. Chem. Soc. Japan,* **42,** 976 (1969).—The effects of carboxylic acids, such as formic, chloroacetic, acetic, propionic, butyric and caproic acid, on the extraction of europium with benzoyltrifluoroacetone were studied. The extraction is enhanced by the adduct formation between metal chelates and carboxylic acids in the organic phase, while it is hindered by the formation of metal-complex ions with anions of carboxylic acids in the aqueous phase. Caproic acid acts as an organic Lewis base and shows the synergism, but formic and chloroacetic acids have a masking effect. Acetic acid, propionic acid, and butyric acid behave both as synergists in the organic phase and as masking agents in the aqueous phase. Caproic acid forms more stable adducts than does *n*-hexyl alcohol, and the composition of the chelate adduct is estimated to be $Eu(BFA)_3 \cdot 2CH_3(CH_2)_4 COOH$.

The Synergistic Effect in Solvent Extraction. The Effect of the Chelating Ligands on the Stability Constant of Lutetium β-Diketonate Adducts with TOPO. T. Honjyo. *Bull. Chem. Soc. Japan,* **42,** 995 (1969).—The steric effect and the inductive effect of the functional groups of β-diketones on the adduct formation between lutetium chelates and TOPO in benzene was studied by using various β-diketones with aliphatic groups (acetylacetone, dipropionylmethane, pivaroylacetone, diisobutyrylmethane and dipivaroylmethane), aromatic groups (benzoylacetone, naphthoylacetone and dibenzoylmethane) and fluoromethyl groups (trifluoroacetylacetone, furoyltrifluoroacetone, thenoyltrifluoroacetone, benzoyltrifluoroacetone and hexafluoroacetylacetone). The effect of the temperature on the adduct formation was then estimated. These results may be summarized as follows: (I) The stability of the adduct increases, and the larger synergism appears, as aliphatic groups, aromatic groups, and fluoromethyl groups are successively substituted for the functional groups of β-diketones. This effect may be due to the electron-withdrawing effect of the fluoromethyl group and the conjugation effect (with a metal chelate ring) of the phenyl group. (2) The adducts contain one molecule of TOPO per metal chelate except for the HFA adduct, which contains two molecules of TOPO. The steric hindrance of the terminal groups is hardly recognizable. (3) The extraction constant of the chelates increases, while the stability of the adducts decreases, with a rise in the

temperature. The apparent enthalpy change ($-\Delta H$ Kcal/mol) upon the adduct formation increases in the order: DPM (5.5) < B_zA (5.9) < BFA (8.6) chelates.

Gas Chromatography of Rare Earth Chelates of Pivaloyltrifluoroacetone. T. Shigematsu, M. Matsui and K. Utsunomiya. *Bull. Chem. Soc. Japan,* **42,** 1278 (1969).—The gas chromatographic behavior of Sc, Y, and rare earth chelates of a new β-diketone, pivaroyltrifluoroacetone (PTA), was investigated. PTA was synthesized by a Claisen condensation from pinacolin and ethyltrifluoroacetone. Sc, Y, Nd, Sm, Eu, Gd, Tb, Dy, Er, Yb, and Lu PTA chelates were prepared. Their elemental analyses and infrared spectra indicated that they were anhydrous tris chelates, and the TGA curves of the chelates proved their good volatile characteristics, showing approximately a 100% weight loss. Gas chromatograms of all the chelates and of mixtures of Sc, Y, and several rare earth chelates were obtained. Some relationships were observed between the retention time, the volatilization temperature, and the ionic radius of the central metal: With the decrease in the ionic radius, the retention time of the chelate decreased and the volatilization temperature became lower.

Fluorometric Determination of Scandium with 5, 7-Dichlorooxine. Y. Nishikawa, K. Hiraki and T. Shigematsu. *Nippon Kagaku Zasshi,* **90,** 483 (1969), in Japanese.—The fluorescent characteristics of the scandium complexes combined with oxine, 5,7-dihalogenooxine (5,7-dichlorooxine, 5, 7-dibromooxine, 5, 7-diiodooxine) and 2-methyloxine were studied to investigate the possibility of fluorometric determination for scandium. As a result, 5, 7-dichlorooxine was found the most effective reagent for scandium determination.

The procedure is as following: To 20 ml of the sample solution containing $\lesssim 10\ \mu$g. Sc^{3+}, 0.25 ml of 0.2% 5, 7-dichlorooxine and 5 ml of 20% ammonium chloride solution were added. The solution was then adjusted to pH 9.5 with aqueous solution of ammonia. The mixture was extracted with 25 ml of chloroform by shaking for 3 min., the organic phase was centrifuged, and the fluorescence intensity of the phase was measured.

The result showed 0.2~10 μg. scandium can be determined within 3% error. The presence of aluminium, yttrium, lanthanum and lutetium introduces positive errors. These hindrances were removed by separating scandium with TTA extraction method, while the determination was not hindered even in the presence of 100 times amount of thorium for 0.5 μg. scandium. This method may be applied to the analysis of rocks and minerals which contain 10^{-3}~10^{-4}% scandium.

Chemical Studies on the Seaweeds (24) Strontium Content in Seaweeds. T. Yamamoto, T. Fujita and T. Shigematsu. *Records of Oceanographic Works in Japan,* **10,** 29 (1969).—The strontium, calcium and magnesium contents in 65 samples of seaweeds of 30 species and 2 samples of limnetic weeds of 2 species were determined by atomic absorption spectroscopy. The method of standard addition was used for strontium and a calibration-graph method for calcium and magnesium.

The strontium content varies in the range from 0.02 to 3.28 ppt with an average of 1.10 ppt in the dry seaweeds (excluding the high values in calcareous seaweed of 9.28, 11.46 ppt). Generally, brown seaweeds have lower values of Ca/Sr atomic ratio than those in other seaweeds and limnetic weeds.

Determination of Lithium in Sea Water by Atomic Absorption. T. Shigematsu, T. Suzuki and M. Tabushi, *Nippon Kaisui Gakkaishi,* **22,** 348 (1969), in Japanese. —Lithium contained in sea water was determined by stomicabsorption spectrophotometry by using air-hydrogen flame. Sodium, potassium and chloride ions so significantly interfered the absorption of lithium that the precise result could not be obtained even when the calibration curve was constructed by addition of lithium standards. Lithium was separated from other alkali metals by extracting the chloride salt with iso-amyl alcohol, and the resulting organic solution was sprayed into the flame. The sensitivity of this procedure was comparatively low, but the reproducibility was much better than in case aqueous solution was used. Thus, more accurate results were obtained. Some sea-water samples were analyzed, and their lithium content was found to be about 140 μg/l in coastal and 170 μg/l in open sea water.

Behaviors of Zinc and Cobalt in Concentrating Process of Sea Water. T. Shigematsu, M. Tabushi and K. Uesugi. *Nippon Kaisui Gakkaishi,* **22,** 351 (1960), in Japanese.—The authors have made a study on the behaviors of minor components in the process of concentrating sea water. The present study dealt with the behaviors of zinc and cobalt ions by using radioactive tracer ^{65}Zn and ^{60}Co.

Zinc and cobalt ions behaved in the similar manner, and indicated a greater loss from the solution evaporated at higher temperature. In contrast with strontium, calcium and phosphate, however, they were never rapidly lost in the final stage of concentration. Therefore, 30–50% of them remained in the solution even after 95% of sea water was evaporated. Most of the zinc and cobalt deposited were distributed in insoluble gypsum deposit, and almost none of them were contained in soluble salt.

Zinc and cobalt in sea water were determined spectrophotometrically with zincone and nitroso R salt, after they were concentrated and separated coprecipitation with aluminium hydroxide. Zinc was concentrated and separated by ion exchange procedure, and cobalt by solvent extraction with dithizone, respectively. As the result of analysis of several sea-water samples, zinc was estimated at 0.3–0.5 μg/l, while cobalt at 4–10 μg/l.

Organic Reagents of Inorganic fluorometric Analysis (I). Y. Nishikawa and T. Shigematsu. *Dotite News Letters,* **17,** No. 2, 2 (1969), in Japanese.—Review.

Trace Elements in Sea Water. T. Shigematsu. *Production & Technique (Osaka),* **21,** 3 (1969), in Japanese.—Review.

Physical Chemistry

Thermodynamic Properties of Galvinoxyl Radical and Its Phenol Derivative; Mechanism of the Phase Transition. Akio Kosaki, Hiroshi Suga and Syuzo Seki. *Bull. Chem. Soc. Japan,* **42,** 1525 (1969). —Measurements of heat capacity of Galvinoxyl radical and its phenol derivative were carried out in the temperature region from 12 to 300°K. Galvinoxyl radical exhibits a phase transition of first-order natur at 81.5°K which corresponds to the susceptibility anomaly already measured.

The enthalpy and entropy of transition amount to 1504.6 J/mol and 18.67 J/(°K·mol), respectively. The entropy change, which corresponds formally to R ln 9.45, cannot be explained by taking only the magnetic contribution. On the other hand, its phenol derivative, the corresponding diamagnetic substance, has not thermal anomaly in the above temperature region. X-ray diffraction patterns at room temperature for both substances agree well with each other in their diffraction angles. From these experimental findings, it seems to be plausible that a kind of transformation of the crystal structure of Galvinoxyl radical takes place at the transition point which may be induced by a pairing of magnetic spins between neighboring molecules.

Solvent Effect on the ESR hyperfine Splitting Constants of Some Phenoxyl Radicals. Y. Oishi, K. Mukai, H. Nishiguchi, Y. Deguchi and H. Takaki. *Tetrahedron Letters,* **No. 46,** 4773 (1968).—The solvent effect on the ESR hyperfine splitting constants of some phenoxyl radicals is studied. The splitting constant of the radical is plotted against the universe of the ionization potential of the solvents. The experimental points fall remarkably close to a straight line.

Electron Microscopic Observation of the Layer of Organo-Montmorillonite. Eiji Suito, Masafumi Arakawa and Tsunoru Yoshida. *Proceedings of the International clay conference,* **1,** 757 (1969).—The layer structure of octadecylammonium-, octadecylammonium-steramide- and trimethyloctadecylammonium-montmorillonite complexes was studied by electron microscopy and selected area electron diffraction.

Lattice images of the layers were observed, which were parallel to the edge of the organo-montmorillonite particles. The observed lattice spacings of the images were 40 Å, 27 Å, 25 Å and 18 Å. Dislocations were often seen in the lattice image and the spacings were sometimes locally different even within one particle.

These results show the non-uniformity of organo-montmorillonite layers, which probably originates from the intrinsic nature of the clay lamellae.

Measurement of specific surface area of powder. Masafumi Arakawa. *Funtai Kôgaku Kenkyukaishi.,* **6,** 31 (1969), in Japanese.—The outline of the measurement of specific surface area of powder is given. The contents are as follows: 1) Adsorption methods. a) Adsorption isotherm, b) Area occupied by one adsorbate molecule, c) Experimental techniques, c)-1 volumetric methods, c)-2 gravimetric methods, c)-3 continuous flow methods, c)-4 liquid-phase adsorption d) Critisism of adsorption methods. 2) Permeametry method. a) Equation for the flow of a fluid through a packed powder bed. b) Experimental techniques and apparatus. c) Critisism of permeametry method.

The n-Donor Complex Formation and Polymorphic Transformation of Zinc Phthalocyanine in Organic Suspension Media. Takashi Kobayashi, Natsu Uyeda and Eiji Suito. *J. Phys. Chem.,* **72,** 2446 (1968).—The polymorphic transformation process of zinc phthalocyanine dispersed in various organic suspension media was studied by x-ray diffraction, differential thermal analysis, and infrared absorption spectroscopy. Strong n-donor solvents, such as heterocyclic and normal amines, dioxane, and dimethyl sulfoxide, were found to form stoichiometric molecular compounds with zinc phthalocyanine in the solid phase. The compositions were

determined by weight-loss measurements and from the thermal behavior of the addition compounds as observed by DTA analysis and x-ray diffraction. The decomposition temperature ranged from 70 to 240°, above which the crystallites were converted into the β form. Solvents other than n-donors caused the α form to undergo an ordinary transformation into the β form. The process was found to be consecutive and two different new polymorphs (χ and θ) appeared as the intermediate phases, depending upon whether the suspension media consisted of electron donors or electron acceptors. The infrared absorption spectra assigned to the fundamental bands of the adduct molecules showed large shifts toward higher frequencies, which suggested that the co-ordination in the complexes could be interpreted in terms of a chargetransfer mechanism.

Elastic and Plastic Deformation of Colloid Gold. Hiroshi Kiho, Saiyu Maruyama and Natsu Uyeda. *Denshi Kenbikyo Gakkaishi,* **17,** 113 (1968), in Japanese. —Deformation in very thin crystal has been studied on laminar crystals of colloidal gold, of about 100Å in thickness and with (III) orientation, grown in dislocations being seldom found.

Prominent elastic bending is often seen. From the estimation of the curvature, it is concluded that the crystals are capable of being deformed elastically as far as the theoretical strength.

At the beginning of plastic deformation, (III) twins are formed mechanically; their thickness is several ten Angstroms being determined from the subsidary maxima of diffraction twin spots. As the deformation proceeds, thickening of twins occurs. (III) slip is also observed.

Crystal Growth from Amorphous Phase in Thin Films. Makoto Shiojiri, Hiroshi Morikawa and Eiji Suito. *Japan. J. Appl. Phys.,* **8,** 1077 (1969).—The crystal growth during crystallization of the amorphous thin films of titanium dioxide and selenium is interpreted. The nucleated crystals grow extending long in a given direction and the interfaces between crystallized and amorphous regions become indented. It is shown that the heat generation at the crystallization and the anisotropic flow of the heat in the crystals lead to these anisotropic growths.

The Porosity Change Based upon Mixing of Fine Powders Having Different Sizes. Masafumi Arakawa and Eiji Suito. *Zairyo,* **17,** 642 (1968), in Japanese. —The packing models such as those devised by Hudson and Horsfield and ordinarily used for mixed powders of different sizes are not applicable to fine powders in which the force of interaction between the powder particles cannot be neglected.

The change of porosity based upon mixing of fine powders having different particle size, was measured. The porosity increased rapidly by addition of small amount of fine powders. However, the porosity seemed to remain constant within certain range by further addition of fine powders. But it increased again when more amount of fine powders were added beyond this range.

The mechanism of this process can be explained by a simple assumption that cohesion of small particles to larger ones increased their points of contact. And the relation between the weight fraction of the small particles added and the increase ratio

of porosity of powder bed in every mixed powder was obtained as

$$\frac{W_s}{f(\varepsilon)\times(W_0-W_s)} = \alpha+\beta\frac{W_s}{W_0}$$

where W_s is the weight of added powder, W_0 is that of total powder mixed and ε is the porosity. The constant β is related to the equilibrium porosity, but the meaning of the constant α is not yet known.

The Flow Property of Powder in Vibrating State. Masafumi Arakawa, Misao Nishino and Eiji Suito. *Zairyo,* **17,** 545 (1968), in Japanese.—The viscosity of powder was measured with the rotational viscometer in a vibrating state. In this experiment, the outer cylinder of Stomer viscometer was tightly connected to the vibrator which had constant frequency (120 cps), and the amplitude was varied by changing the voltage applied to the vibrator. The α-alumina powders with several kinds of particle sizes were used as samples.

The flow curves, obtained for powders of various particle sizes under different amplitudes and temperatures, were found to be similar to those of non-Newtonian liquids. When the amplitude decreased, each powder behaved like a continuous solid.

The apparent viscosity was obtained from these flow curves in relation to the different amplitudes and particle sizes. At a constant rate of shear and large amplitude, the apparent viscosity decreased with decrease in particle size. When the amplitude was sufficiently small, the apparent viscosity reached its minimum at a definite particle size. It was considered that in the fine powders their coagulated secondary particles moved as flow units, and that these coagulated particles were broken into primary particles with increase of amplitude.

The Effect of Temperature upon the Adhesive Properties of Powder. Misao Nishino, Masafumi Arakawa and Eiji Suito. *Zairyo,* **18,** 535 (1969), in Japanese. —Some properties of powder beds, *i.e.* "viscosity" of powder in a vibrating stage, their packing density, the angle of repose and shearing stress, were measured at a range from room temperature to about 300°C. α-alumina powders with several kinds of particle sizes and spherical glass powder were used as the samples.

Increasing the temperature in the range higher than 100°C, in which moisture was considered not to be effective upon the adhesive properties of these powders, the "viscosity" and the angle of repose increased and the packing density decreased. These results suggest that the attractive force between the particles increases with the increase of temperature as has been verified by the shearing tests.

The theoretical calculation of sedimentation volume, which was studied by Nakagaki *et al.* for the packing density in relation to the adhesive probability of particles, P, was applied to the packing density in a heated state in order to obtain the quantitative relation between the attractive force and temperature. On the basis of an assumption that P was given as a function of $k\alpha D/mv$, where k, α, D, m and v were respectively shape factor, temperature factor, particle size, mass of the particle and sedimentation velocity of particle in hot air, the relation between α and absolute temperature T was obtained in the following equation.

$$\log\alpha = {}_a T/T_m - b$$

In this equation, T_m was the absolute temperature of melting point of the sample. The constant a was found to be the same one for α-alumina and glass powder.

The effects of temperature upon the angle of repose and the "viscosity" of powder were systematically interpreted in terms of the temperature factor α obtained from the above equation.

Electron Microscopic Studies on Inorganic Materials (Review). Eiji Suito. *Ceramics*, **3,** 443 (1968), in Japanese.—Recent developments of electron microscop and its application to inorganic materials are reviewed. The contents are as following: 1) high resolution electron microscope, 2) high voltage electron microscope, 3) new techniques for sampling, 4) scanning electron microscope, 5) application to inorganic materials (a) raw materials for ceramics-clay minerals (b) powdery materials (c) sintered materials (d) natural jewels and (e) synthesized minerals.

Packing structure of fine Powder. Masafumi Arakawa. *J. Japan Soc. Powd. Powd. Metall.*, **15,** 55 (1968), in Japanese.—Bulkiness of powder was studied to determine the relationship between particle size and cohesiveness. The variation of the void volume of powder beds with particle size, and the change of porosity with mixtures of various particle sizes were measured. Results suggested that the packing process of powders is determined in relation to particle gravity and cohesive force at a contact point between particles. The cohesive force at a contact point was also measured by shearing tests of powder beds of various particle size. It was observed that the fine particles form scaffold structure in the aggregated state, confirmed by a model experiment with foaming polystylene particles.

Solvent Effect on the Transformation of Crystalline Powders in Organic Suspensions. Natsu Uyeda. *Kagaku to Kôgyô,* **22,** 110 (1968), in Japanese.—The behavior of organic crystalline powders were discussed in terms of charge transfer properties of powders and suspension media.

Two papers were reviewed in Japanese.

1) Eiji Suito, Natsu Uyeda, *Kolloid-Z.* **193,** 97 (1963).
2) T. Kobayashi, N. Uyeda, E. Suito, *J. Phys. Chem.*, **72,** 2446 (1968).

The State of Trimethyloctadecylammonium·Steramide Complexes Adsorbed on Bentonite. Tsunoru Yoshida, Masafumi Arakawa and Eiji Suito. *Kôgyô Kagaku Zasshi,* **71,** 820 (1968), in Japanese.—The complexes of trimethyloctadecylammonium·steramide (TMODA·SA) and trimethyloctadecylammonium (TMODA) with bentonite were studied by x-ray diffraction and differential thermal analysis (DTA).

(TMODA)-bentonite shows stepwise increments of 4Å in basal spacing with increasing organic contents. (TMODA·SA)-bentonite shows mixed layer structures in which basal spacings were 19Å and 12.5Å at organic contents of 90-meq-(TMODA·SA)/100g-clay and 19Å, 15.5Å and 12.5Å at organic contents of 150 meq-(TMODA·SA)/100 g-clay.

The DTA curves of (TMODA·SA)-bentonite show two endothermic peaks at 60°C and 78°C, but TMODA-bentonite has no DTA peak at those temperature ranges.

From the interpretation of peak area of the DTA peaks, it was concluded that

SA and TMODA or TMODA-chloride adsorbed on the external surface of bentonite have made two-dimensional order structure.

Electrocapillary Phenomena at Oil-Water Interfaces. Part III: The Behavior of Lecithin at Oil-Water Interfaces. A. Watanabe, M. Matsumoto, H. Tamai and R. Gotoh. *Kolloid-Z.,* **228,** 58 (1968).—The interfacial tension, between the oil phase containing an ionic surface active agent and the aqueous phase containing an inorganic electrolyte, is a function of the potential difference applied to the two phases from an outer circuit. This phenomenon, the electrocapillarity at oil-water interfaces, was used by the present authors to study the structure of electrical double layers and the interaction between surface active agent ions and counterions. In the present study an amphoteric material, the lecithin, was used as the surface active agent, and its adsorption and dissociation behaviors as well as its interaction with counterions were examined. It was found that the lecithin dissolved in the "oil" phase behaved as the cationic or anionic surface active agent according as the pH of the "aqueous" phase was acidic or alkaline. This showed that the ionic groups of the lecithin molecule are immersed into the aqueous side of the interface. Since the interfacial tension was independent of the applied potential at the interfacial isoelectric point, this point could be measured with a high sensitivity. The ionic species of the inorganic electrolyte in the aqueous phase had a marked influence on the isoelectric point. The reversal of charge spectra thus obtained were found to agree fairly well with that obtained by other authors using electrophoretic measurement.

The Interaction between Surfactants and Dyestuffs at Oil-Water Interfaces. A. Watanabe, H. Tamai, M. Matsumoto and R. Gotoh. *Nippon Kagaku Zasshi,* **90,** 738 (1969), in Japanese.—The interaction between surfactant and dyestuff at the oil-water interface, and the influence of inorganic electrolyte on it, were studied by measuring the electrocapillary curve.

When the oil phase contained the cationic surfactant, or the amphoteric surfactant (for the acidic aqueous phase), and the aqueous phase contained the anionic dyestuff, the depression of the interfacial tension over the cathodic polarization range, which had been found to be characteristic to cationic surfactants, was suppressed by the binding of the surfactant and dyestuff at the interface. However, if the aqueous phase contained the anionic dyestuff, *e.g.* Benzopurpurin 4B, no binding was found to take place and the ordinary builder effect, *i.e.* the increase in surface activity, was observed.

When the oil phase contained the anionic surfactant, or the amphoteric surfactant (for the alkaline aqueous phase), and the aqueous phase contained the cationic dyestuff, the depression of interfacial tension over the anodic polarization range was suppressed by the dyestuff-surfactant binding.

It was also found that these bindings were strongly dependent on the species and concentration of the electrolyte in the aqueous phase.

Recent Advances in the Infra-Red Spectroscopy of Adsorbed Molecules. N. Sheppard, N. R. Avery, M. Clark, B. A. Morrow, C. Smart, T. Takenaka, and J. W. Ward. *"Molecular Spectroscopy", Edited by P.Heppel, The Institute of Petroleum,* **97,** (1968).—This paper gives a review of certain selected topics in the field of the infra-red spectra of adsorbed molecules.

The paper is firstly concerned with the experimental techniques used to obtain absorption spectra from various types of high area absorbents. In addition, progress to date and future prospects are discussed of work on evaporated metal films and for emission studies of adsorbed molecules.

Typical spectra and their interpretation are discussed for chemisorbed ethylene on Pt, Pd, and Ni, butene-1 on Pt and Ni, and benzene on Pt. Although the interpretation of such spectra in terms of the structures of the adsorbed species is a difficult matter, this can be achieved in a number of cases with the help of spectra studied at various temperatures, changes in the spectra resulting from hydrogenation, and spectra of isotopically substituted species. Most of the spectra obtained from ethylenes and substituted ethylenes can best be interpreted in terms of hydrocarbon groupings σ-bonded to the metal surface. Those obtained from aromatic molecules are consistent with π- or σ-bonding interpretations.

What is Electronegativity? Tohru Takenaka. *Kagaku,* **24,** 394 (1969), in Japanese.—This paper is a review article of electronegativity which has been proposed first by Pauling as "the power of an atom in a molecule to attract electrons to itself".

The various definitions of electronegativity are given in detail and are interpreated on the basis of the quantum chemistry. The relationships are discussed between electronegativity and various types of physical properties in a molecule, such as the bond dipole moment, the percentage ionic character of a bond, the nuclear quadrupole coupling constant, the chemical shift in the NMR spectra, the equilibrium bond length of polar bonds, and the force constant and frequency of the molecular vibrations.

Lastly, the methods of measuring the group electronegativity of a radical are given and the numerical values obtained are compared with the calculated values given by taking account of the state of hybridization and the effect of the electronegativity property of other atoms on the bonding atom in the radical.

Dielectric Properties of Polytetrafluoroethylene and Tetrafluoroethylene-Hexafluoropropylene Copolymer. N. Koizumi, S. Yano and F. Tsuji. *J. Polym. Sci., Part C,* **23,** 499 (1968).—Precision measurements of dielectric properties of polytetrafluoroethylene and copolymers of tetrafluoroethylene and hexafluoropropylene were made over a temperature range of -40 to $+180$°C at frequencies of 10 Hz to 300 kHz. Polytetrafluoroethylene exhibited the typical dielectric behavior of a nonpoar substance: no dielectric loss peak was found over the experimental range of temperature and frequency. The dissipation factor remaines constant, being about 2×10^{-5}. Copolymers of tetrafluoroethylene and hexafluoropropylene showed two dielectric loss peaks : one occured at about 100°C. and the other at about -20°C. There was a break point, or an abrupt bend, near 60°C. in the curve of dielectric constant versus temperature, indicating the existence of a transition point. The high- and low-temperature loss peaks correspond to the α and γ relaxations, respectively, which have been found for the mechanical behavior of this copolymer. The dielectric relaxation in the copolymer was attributed to the slightly polar nature of the perfluoromethyl side groups. The activation enthalpy and entropy are 80 kcal./mole and 180 eu for the α relaxation and 12 kcal./mole and 15 eu for the γ relaxation, respectively. The α

and γ relaxation are discussed in connection with the molecular motion of the copolymer chain.

Dielectric Relaxation of Poly(vinylidene fluoride). N. Koizumi, S. Yano, and K. Tsunashima. *J. Polym. Sci., Part B,* **7,** 59 (1969). —Dielectric properties of poly (vinylidene fluoride) were studied over a temperature range of −195 to 160°C at frequencies between 10 Hz and 300 kHz. Three dielectric relaxations, α, β, and γ, were observed near 80, −20 and −80°C at 1 kHz, respectively. With increasing crystallinity the dielectric loss maximum ε''_{max} in the α relaxation increased in magnitude and shifted to higher temperature, while in the β relaxation ε''_{max} was depressed with increasing crystallinity and the temperature at which ε''_{max} occurred was almost independent of crystallinity. In drawn samples which had the β-type crystal structure ε''_{max} in the α relaxation decreased markedly in spite of relatively high crystallinity. This effect was attributed to an anisotropic structure in the crystalline regions produced by drawing. Thus the molecular motion in the crystalline regions was responsible for the α relaxation. The β relaxation was assigned to micro-Brownian motions of the molecular chain in the amorphous regions, since the relaxation took place above the glass transition temperature and the temperature dependence of relaxation times was of the WLF type.

Inorganic Chemistry

Magnetic Properties of Organic Stable Radicals. I. 2,2,6,6-Tetramethyl-4-Hydroxypiperidine-1-Oxyl. Jun Yamauchi, Teruaki Fujito, Eiji Ando, Hiroaki Nishiguchi and Yasuo Deguchi. *J. Phys. Soc. Japan,* **25,** 1558 (1968). —The static magnetic susceptibility and the ESR absorption spectra of 2,2,6,6-tetramethyl-4-hydroxypiperidine-1-oxyl in the temperature range from 1.8°K to 300°K have been measured. This powder sample shows a braod maximum in the susceptibility at the temperature 6.5°K. It has been shown that the temperature dependence of the susceptibility is fitted better by the one-dimensional Heisenberg model than the linear Ising model or a singlet-triplet model. The Curie-Weiss constant and the exchange interaction energy along the chain are estimated to be −6.0°K and −5.0°K, respectively. The linewidth of the ESR absorption spectra increases rapidly as decreasing temperature below 6.5°K.

Magnetic Properties of the hcp Iron-Ruthenium Alloys. Hideo Ohno, Mamoru Mekata and Hideo Takaki. *J. Phys. Soc. Japan,* **25,** 283 (1968).—The magnetic properties of the hcp Fe_{1-x} Ru_x (0.15×0.3) alloys were studied by Mössbauer effects of Fe^{57}. At low temperatures, a broadened line was observed, showing an antiferromagnetic ordering.

The internal field at 6°K and the Néel temperature were 15KG and 100°K, respectively, and almost concentration independent.

Spectra of uv-Induced Absorption in Alkaline-Earth Tungstates. S. Sakka. *J. Appl. Phys.,* **39,** 4863 (1968). —Absorption spectra were determined for uv-colored alkaline earth tungstate compounds and solid solutions of the compositions

Ca_{1-x} Sr_x WO_4 and Sr_{1-x} Ba_x WO_4, where $x = 0$-1, all doped with 0.1 % Bi. Comparison of the spectra indicated a correlation among the absorptions of the samples different in composition; in the visible region there were three series of absorption bands and the peak positions of these bands varied systematically with composition. The good correlation between composition and peak wavelength for each series of bands suggests that the nature of the color centers may be the same for all compositions. The plot of peak wavelength against lattice constant indicated that the peak wavelength decreases with increasing lattice constant for every series of bands. This observation is surprising, for the direction of the change in peak wavelength is opposite to what was expected from the data on the absorption of the color centers in alkali halides. It is known that in alkali halides peak wavelength of all the color centers, whether they are electron-trapping centers or holetrapping centers, increases with increasing lattice constant. The development of the theoretical consideration, which will enable explanation of the "unusual" dependence of the peak wavelength for tungstates upon lattice constant is awaited.

High Pressure Effects on Glass. S. Sakka and J. D. Mackenzie. *J. Non-Crystalline Solids*, **1,** 107 (1969).—The application of high pressure at different temperatures can produce many anomalous and interesting results. This paper is a comprehensive review of the effects of high pressure on glass. While the major portion of this review is concerned with "glass", that is, systems at temperatures below the glass transition temperature T_g, some attention is also paid to "molten glasses" at higher temperatures. The contents are as follows:

1. Introduction
2. High pressure devices
3. Densification
   - 3.1. *Compressibility*
   - 3.2. *Densification in rigid state*
     Effects of shear
     Densification by hydrostatic pressure
     Effect of composition,
     Stability of densified glass,
     Structural changes on densification
   - 3.3. *Densification in non-rigid state*
4. Crystallization
   - 4.1. *Review of some experiment*
   - 4.2. *Theory of the effect of pressure*
   - 4.3. *Experiments on* SiO_2 *and* B_2O_3 *glasses*
5. Electrical properties
   - 5.1. *Glass with ionic conduction*
   - 5.2. *Semiconducting glass*
6. Viscosity of glass
7. Optical properties
   - 7.1. *Absorption spectra of transition metal ions*
   - 7.2. *Color centers*
8. Miscellaneous
   - 8.1. *Gas solubility at high pressure*
   - 8.2. *Reduction of ions*
   - 8.3. *Indentation hardness*
   - 8.4. *Glass forming polymer and organic compounds*
   - 8.5. *Surface compression*

Colloids in Glass: Photosensitive and Photochromic Glasses. S. Sakka. *Hyomen*, **7,** 227 (1969), in Japanese.—Both photosensitive and photochromic glasses are colloidal systems with, respectively, noble metal (gold, silver and copper) and silver (or thallium) halide fine particles of the size ranging from about 50 Å to 1000 Å incorporated in glassy matrix. Characteristic properties of these two glasses have been reviewed mainly from scientific aspects.

As to photosensitive glass, the mechanism of formation of silver colloids has been

described in detail on the basis of optical measurements conducted in the author's laboratory. Upon UV irradiation of glass an electron is trapped by a Ce^{4+} ion, forming complex. This complex traps a silver ion and then another electron when the glass is heated at 150-200°C. At about 200-350°C the similar process is repeated and leads to the formation of a latent image consisting of three or four silver atoms. Above 350°C the latent image grows to a silver colloid particle. Change of optical absorption by silver colloids and their efficiency in nucleating silicate crystals were also discussed as a function of the particle size of silver colloids.

Regarding photochromic glass, the effect of ambient temperature on the darkening and fading and the effect of long wavelength light on fading (optical bleaching) have been described using the data on TlCl-containing photochromic glasses discovered by the author (S. Sakka and J. D. Mackenzie, New Phototropic Glasses, 8th Intern. Congress on Glass, Paper 145, London (July, 1958)). Also it was demonstrated that comparison of darkening and fading characteristics of silver halide or thallium halide crystallites incorporated in glass with those of corresponding single crystals is important for developing the theory of photochromic coloration of glasses.

Finally, industrial applications of these glasses have been discussed briefly.

Colors of Glasses Produced by Transition Metal Ions. T. Yamamoto. *Kagaku to Kôgyo,* **43,** 57 (1969), in Japanese.—Various aspects of coloration of glasses based on transition metal ions have been reviewed. Ligand field theory and its application to colored glasses have been explained. In glasses equilibrium between oxidation and reduction states of a transition metal ion changes sensitively in terms of chemical composition of base glass, melting atmosphere, melting temperature and concentration of the transition metal. The change of equilibrium was demonstrated with iron ion as an example. High pressure effect on glasses containing cobalt ion was also discussed.

Phototropy of Alkaline Earth Tungstates Doped with Bismuth. S. Sakka. *J. Amer. Ceram. Soc.,* **52,** 69 (1969).—In the course of the study on phototropic materials it was found that calcium, strontium, and barium tungstates and their solid solutions, doped with a small amount of bismuth, color remarkably on exposure to ultraviolet light and return to the original white state by thermal fading or optical bleaching. The factors affecting the darkening and fading processes were investigated experimentally. Under the same irradiation conditions the intensity of uv-induced coloration depended on the Bi content and preparation temperature of the tungstates. Bi contents higher than 0.1 mole % and preparation temperatures higher than 1250°C gave strong coloration. The rate of fading of uv-induced color increased with increasing Bi content. The fading was accelerated by heating; almost all the uv-induced color disappeared at 230°C in 30 minutes. The apparent activation energies for the thermal fading process were 0.08 to 0.20 ev, depending upon the Bi content. These values of activation energy appeared to suggest that the nature of the defect inducing the color is trapped electron or trapped hole center. The fading rate was also increased by visible light exposure. The uv-induced absorption spectra varied systematically with the composition of the tungstates, and the peak wavelength of the three series of absorption band decreased with increasing lattice constant of tungstate crystal.

The Trend of Glass-Ceramics Research. Megumi Tashiro. *Ceramic Data Book, 337* (1969), in Japanese.—The trend of glass-ceramics research was reviewed. Glass-ceramics which have been developed up to date were classified in terms of their chemical compositions. The characteristics and the problems to be solved were shown for each of them. Newly developed glass-ceramics, such as a neutron-absorbing glass-ceramics and metal-sealing glass-ceramics, were also referred to. Crystallization process of glass was discussed with particular emphasis on the initial stage of the crystallization of Li_2O-SiO_2 glasses.

Effects of the Addition of Fluorine on the Surface Structure of Glass-Ceramics. Tohru Kanbara and Megumi Tashiro. *Yôgyô Kyôkai shi,* **76,** 385 (1968). —In order to investigate the causes of the increase in the modulus of rupture of low-expansion glass-ceramics in the system Li_2O-Al_2O_3-SiO_2 by the addition of fluorine, surface and internal microstructures of specimens containing various amount of fluorine were examined by x-ray diffraction method and electron microscopic observation. The causes were attributed to the following two factors: (1) Marked decrease in the thickness of the glassy layer on the surface of glass-ceramics; depth of Griffith flaw on the surface would be reduced. (2) Formation of β-quartz ss crystallites together with β-spodumene ss crystallites at the surface of the glass-ceramics with the addition of a large amount of fluorine; presence of β-quartz ss crystallites with low thermal expansion coefficient would induce a compressive stress at the surface.

Internal Magnetic Field at Fe^{57} in Hexavalent States. Teruya Shinjo, Toshio Ichida and Toshio Takada. *J. Phys. Soc. Japan,* **26,** 1547 (1969).—Mössbauer results of three hexavalent iron compounds, K_2FeO_4, $SrFeO_4$ and $BaFeO_4$ were presented. K_2FeO_4 and $BaFeO_4$ showed the antiferromagnetic splitting at low temperatures and the internal field of hexavalent iron was found to be about 130kOe. $SrFeO_4$ was paramagnetic even at 2°K.

Magnetic Properties of Jarosites, $RFe_3(OH)_6(SO_4)_2$ (R=NH_4, Na or K). Mikio Takano, Teruya Shinjo, Masao Kiyama and Toshio Takada. *J. Phys. Soc. Japan,* **25,** 902 (1968).—The Mössbauer experimental results on three jarosite compounds were reported. At 300°K and 80°K the spectra of all these compounds were paramagnetic and the symmetric doublets due to quadrupole interaction were observed. At 4.2°K, well resolved six lines appeared and the magnetic orderings were confirmed. The results of magnetic susceptibility measurements were also presented.

Growth of Co_3O_4 single crystals and Its Reaction Mechanism. T. Takada, Y. Bando, N. Yamamoto and K. Nagasawa. *Japan, J. Appl. Phys.,* **8,** 619 (1969).—This note reports the condition of the growth of Co_3O_4 single crystals and the reaction mechanism of Co_3O_4 in a closed system. After the quartz tube in which Co_3O_4 powder was included was evacuated to 10^{-6} mm Hg, HCl gas was introduced into this tube. Then this tube was sealed off. It was horizontally placed in a furnace having a temperature gradient (800°C to 1000°C). Transport of Co_3O_4 by HCl has yielded some black, bright crystals of octahedral shape. The reaction mechanism of Co_3O_4 was discussed.

Growth of VO_2 Single Crystals by Chemical Transport Reaction. Y. Bando, K. Nagasawa, Y, Kato and T. Takada. *Japan. J. Appl. Phys.*, **8,** 633 (1969). —This note reports a new method for growing VO_2 single crystals and their electrical property. The single crystals were prepared by chemical transport reaction in the closed system using tellurium tetrachloride $TeCl_4$ as transport agent. The tube containing sintered VO_2 and $TeCl_4$ was evacuated to 10^{-6} mm Hg and sealed off. The tube was horizontally placed in the furnace having a temperature gradient. VO_2 single crystals were deposited at the colder zone. Two kinds of crystals different in shape were obtained in the same tube. The electrical conductivity along the longitudinal direction of rod-like crystals was measured by four point method. It was observed that the transition temperature from simiconductive to metallic state was about 67°C and that there was a jump in the conductivity of five orders of magnitude.

Formation and Physical Properties of Iron Oxides and Hydroxides. T. Takada. *Denki Kagaku,* **37,** 328 (1969), in Japanese.—The physical properties and formation of iron oxides (FeO, Fe_3O_4, α-Fe_2O_3, γ-Fe_2O_3) and hydroxides ($Fe(OH)_2$, Green Rust, α,β,γ-FeOOH, Jarosite) were reviewed.

(1) The properties

Shape and size of particles obtained from aqueous solution were reviewed and their effects on physical properties were elucidated. $Fe(OH)_2$, $Fe(OH)_2$·FeOOH, α-,β-,γ-FeOOH and Jarosite are antiferromagnetic. Néel temperature and direction of spin axis are experimentally determined by magnetic and Mössbauer measurements.

(2) Formation

Iron oxides and hydroxides were mainly prepared from aqueous solution, and mechanisms of preparation were discussed.

The role of Impurity in Sintering of Oxides. Y. Bando. *J. Japan Soc. Powd. Powd. Metall.*, **15,** 414 (1969), in Japanese.—The investigation on sintering of oxides containing minor amounts of impurites were reviewed. Impurites in oxides were frequently found to locate at grain boundaries by means of x-ray microanalyser, autoradiograph, and dispersion of electricity. Grain-boundary segregation of impurities occurred by liquid phase sintering when the ferrite containing CaO and SiO_2 was sintered. In the case of minor amount of liquid, the grain growth was discontinuous.

Mössbauer Effect of Fe^{57} in CrO_2. Teruya Shinjo, Toshio Takada and Nobuaki Tamagawa. *J. Phy. Soc. Japan,* **26,** 1404 (1969).—Samples of CrO_2 containing a small quantity of Fe^{57} were prepared and the Mössbauer effect was measured at various temperatures. It was found that Fe atoms were dissolved in CrO_2 taking the electronic state of trivalent ion. The temperature dependence of the internal magnetic field at Fe was analyzed by using a simple molecular field approximation and the coupling between Fe and Cr was discussed. The spin direction of Fe was determined to be antiparallel to the magnetization of CrO_2 matrix by the Mössbauer measurement in an external magnetic field (45 kOe).

Mössbauer Effect Study in Cu-2%Co Alloy: The Transformation of Precipitates Induced by Cold Rolling. Saburo Nasu, Yotaro Murakami, Yoji

Nakamura and Teruya Shinjo. *Scripta Metallurgica,* **2,** 647 (1968).—For the detailed investigation of the precipitation phenomena in Cu-2%Co alloy, the Fe^{57} Mössbauer effect study has been made using the specimen doped with Co^{57}. The specimen was heavily rolled and the spectra were obtained as a function of thickness reduction. The fcc→hcp transformation of precipitated Co particle was observed when the reduction was heavier than 70%. The change of the internal magnetic field was also reported.

Iron Impurities in the Antiferromagnetic Manganese Copper ($Mn_{0.95}Cu_{0.05}$) Alloy. Yasuo Endoh, Yoshikazu Ishikawa and Teruya Shinjo. *Physics Letters,* **29A,** 310 (1969).—Magnetic and electric properties of $Mn_{0.95}Cu_{0.05}$ and $(Mn_{0.95}Cu_{0.05})_{0.99}Fe_{0.01}$ alloys have been investigated over a temperature range from 4.2°K to 600°K. Mössbauer measurements were made at 4.2°K in the presence of external magnetic fields up to 50kOe. The results suggested that the iron atom in the antiferromagnetic γ manganese has no localized moment.

The Use of the Mössbauer Effect. Teruya Shinjo. *Hyômen,* **6,** 732 1968, in Japanese.—A brief introduction of the Mössbauer effect is presented and two recent topics are described. The first topic is concerned with the relation between the Mössbauer spectrum and the particle orientation. With the samples consisting of oriented particles, the magnetic spin directions are estimated. Here it is suggested that the Mössbauer effect is a useful means for the observation of particle orientation. The second topic is the study of surface behavior. The atomic motions of Sn atoms adsorbed on silica gels are microscopically studied.

Application of Mössbauer Spectroscopy. Teruya Shinjo. *J. Japan Soc. Powd, Powd. Metall.*, **15,** 7 (1969), in Japanese.—Three Mössbauer studies were presented here.

(1) Using the samples of oriented particles for the absorbers of Mössbauer effect, the magnetic spin direction was estimated.

(2) In order to study the catalysis reaction, the Mössbauer spectrum of Fe atoms in Al_2O_3 was investigated. The processes of reduction and oxidation were repeated and the behavior of Fe atoms in Al_2O_3 was microscopically elucidated.

(3) It was suggested that the backscattering Mössbauer measurement was useful for the study of surface behavior. For an example, results of oxidized steel were introduced.

Mössbauer Effect Study of α-FeOOH and β-FeOOH: Making Use of Oriented Particles. Naoichi Yamamoto, Teruya Shinjo, Masao Kiyama, Yoshichika Bando and Toshio Takada. *J. Phy. Soc. Japan,* **25,** 1267 (1968).—Mössbauer absorption spectra were measured for oriented samples of α- and β-FeOOH particles at antiferromagnetic and paramagnetic states, which were prepared utilizing the anisotropic particle shape. Considering the intensity ratio of six absorption peaks, the direction of the electron spin in antiferromagnetic state was concluded to be parallel to crystal c-axis in each compound. From the intensity ratio of paramagnetic quadrupole doublet, the electric field gradient was discussed. The gradient axis of β-FeOOH was estimated to be in *c*-plane.

Organic Chemistry

Terpenoids. IX. The Structure and Absolute Configuration of Isodocarpin, a New Diterpenoid from *Isodon trichocarpus* Kudo and *I. japonicus* Hara. Eiichi Fujita, Tetsuro Fujita, and Masayuki Shibuya. *Chem. Pharm. Bull. (Tokyo),* **16,** 1573 (1968).—A new diterpenoid, which was named isodocarpin, was isolated from the dried leaves of *Isodon trichocarpus* Kudo and *I. japonicus* Hara. Its molecular formula was found to be $C_{20}H_{26}O_5$. The presence of a five-membered ring ketone which was conjugated with an exocyclic methylene group was supported from the IR and UV absorptions and the NMR spectral data. The NMR spectrum closely resembled that of enmein. The detailed spectroscopic investigation led to a postulation that isodocarpin may be 3-deoxyenmein. The chemical conversion of enmein into dihydroisodocarpin confirmed that the above assumption was correct.

On the Stereoisomers of Some Enmein Derivatives. Eiichi Fujita, Tetsuro Fujita, Yoshimitsu Nagao, p. Coggan, and G. A. Sim. *Tetrahedron Letters,* **No. 39,** 4191 (1968). —This communication deals with the synthesis of possible four epimeric alcohols from enmein, the major diterpenoid of *Isodon* species, and the assignment of their structure and absolute configuration. Spectroscopic and chemical evidence allowed to propose their stereochemistry. It was recognized by x-ray analysis carried out by Coggan and Sim on the bromoacetate of one epimer that the structural and stereochemical assignments to the four epimers were correct.

Diterpenoids of "Enmeiso" (*Isodon japonicus* Hara and *I. trichocarpus* Kudo). Eiichi Fujita. *Ten'nenbutsu Kagaku '68 (Kagaku no Ryoiki Zokan, 86),* 173 (1968), in Japanese. —This is a review which deals with the research works on the diterpenoids of *Isodon japonicus* Hara and *I. trichocarpus* Kudo mainly carried out in our laboratories from 1963 to 1968.

Further Evidence for the New Skeleton of Lythrum Alkaloids. Eiichi Fujita, Kaoru Fuji, and Kunihiro Tanaka. *Tetrahedron Letters,* **No. 56,** 5905 (1968). —The structures of lythranine, lythranidine, and lythramine, alkaloids isolated from *Lythrum anceps* Makino, had been proposed by the authors. They presented unambiguous evidence for the new skeleton of these natural products. Eight steps of reactions gave the expected macro-ring compound which contains a pyridine nucleus. The synthesized product was proved to be identical with a compound derived from lythranidine. Thus, the previously proposed structures of the alkaloids were recognized to be correct.

Terpenoids—X. Chemical Conversion of Enmein into Enantio-abietane and Total Synthesis of Abietane. E. Fujita, T. Fujita, H. Katayama, and Y. Nagao. *Tetrahedron,* **25,** 1335 (1969).—The acyloin condensation of a lactone ester derived from enmein, a diterpenoid bitter principle from *Isodon trichocarpus* Kudo, was investigated. The acyloin products were converted into a three cyclic saturated hydrocarbon through several steps of reactions, while abietic acid was transformed into its skeletal hydrocarbon. The both compounds were proved to be enantiomeric with each other. We proposed the name "abietane" for the latter hydrocarbon, hence "*enantio*-abietane"

for the former. Since abietic acid had been synthesized, its conversion into abietane constituted the total synthesis of the latter.

Terpenoids—XI. The Structure and Absolute Configuration of Trichokaurin and Its Chemical Conversion into (−)-Kaurene and Diterpene Alkaloids. E. Fujita, T. Fujita, M. Shibuya, and T. Shingu. *Tetrahedron,* **25,** 2517 (1969).—The structure and absolute configuration of trichokaurin, a diterpenoid of *Isodon trichocarpus* Kudo, have been established on the basis of spectral and chemical evidence. The chemical conversion of trichokaurin into *ent*-16-oxo-17-norkauran-20-oic acid has been accomplished, which means the transformation of trichokaurin into (−)-kaurene, atisine, garrying, and veatchine.

The Chemical Conversion of Enmein into *ent*-15-Kaurene and *ent*-16-Kaurene. Eiichi Fujita, Tetsuro Fujita, Yoshimitsu Nagao, Hajime Katayama, and Masayuki Shibuya. *Tetrahedron Letters,* **No. 30,** 2573 (1969).—The acyloin condensation with an unsaturated lactone ester derived from enmein was repeatedly carried out. The investigation of the reaction condition led to a success in getting a desired compound as a major product. The key compound was converted into *ent*-15-kaurene and *ent*-16-kaurene through several steps of reactions including Jone's oxidation and Wolff-Kishner reduction.

Formal Chemical Conversion of Enmein into *ent*-Kaurene, Atisine, Garryine, and Veatchine. Eiichi Fujita, Tetsuro Fujita, and Hajime Katayama. *Tetrahedron Letters,* **No. 30,** 2577 (1969).—This communication described the chemical transformation of enmein, a major diterpene of *Isodon* species, into the known hemiacetal diol. Since the latter had been connected chemically to *ent*-kaurene, atisine, garrying, and veatchine, a formal chemical conversion of enmein into them was performed. In a sequence of reactions, an interesting acetyl migration was observed and a good yield of the photochemical oxygenation was obtained.

The Synthesis of Methylacetylene by the Pyrolysis of Propylene. IV. The Pyrolysis of Allyl Chloride. S. Kunichika, Y. Sakakibara and M. Taniuchi. *Bull. Chem. Soc., Japan,* **42,** 1082 (1969).—Allyl chloride has been pyrolyzed in a flow system over a wide range of conditions (temperature, 800–1200°C; contact time, $0.665\times10^{-3}-78.9\times10^{-3}$ sec; concentration, 4.0–13.5 mol%; pressure, atmospheric pressure) to find suitable conditions for producing methylacetylene and allene. In addition, a study on the mechanism of pyrolysis of allyl chloride at high temperatures (800–1200°C) has been made. A total yield of allene and methylacetylene of 14 mol per 100 mol of allyl chloride pyrolyzed was obtained under suitable conditions. By means of the zero conversion method, hydrogen propylene, allene, diallyl, 1,3-cyclohexadiene, and benzene have been found to be the main reaction products in the early stage of the pyrolysis, while methane, acetylene, ethylene, methylacetylene, butene-1, and butadiene have been found to be the side reaction products. The over-all activation energy of decomposition was 39.4 kcal/mol for an A factor of $10^{8.7}$ sec^{-1}. On the basis of the observed results, a free-radical mechanism has been proposed for the main reactions and the principal side reactions. It was further

concluded that the pyrolysis was a radical decomposition initiated by the reaction $C_3H_5Cl \rightarrow C_3H_5\cdot + Cl$ and that the over-all mechanism in the early stage of the pyrolysis was represented essentially by the reaction $2C_3H_5Cl \rightarrow C_3H_5\cdot + \dot{C}_3H_4Cl + HCl$.

Kinetic Study on the Addition Reaction of Carbon Monoxide with Ethyl Fluoride under High Pressures. Makoto Kanbara, Nobuyuki Sugita, Hiroshi Teranishi and Yoshimasa Takezaki. *Bull. Japan Petrol. Inst.*, **11,** 48 (1969).—The reaction of carbon monoxide with ethyl fluoride has been investigated in the anhydrous hydrogen fluoride medium under high pressure.

The yield of propionic acid was fairly high, for instance, 89 mole % yield to the charged ethyl fluoride in 3 hrs under the conditions: CO pressure 600 kg/cm^2 and charged mole ratio (HF/C_2H_5F) 42.

The rate of formation is of the first order with respect to the pressure of carbon monoxide and one half to the charged mole ratio of hydrogen fluoride and ethyl fluoride.

The overall activation energy is 6.9 kcal/mole.

Leaf alcohol XVIII. Condensation of Leaf Aldehyde by Means of Diethylamine. T. Kajiwara, A. Hatanaka, Y. Inouye and M. Ohno. *Agr. Biol. Chem.*, **33,** 409 (1969).—The diethylamine-catalyzed aldol condensation of *E*-2-hexenal yielded a mixture of 2-*E*, 4-*E*-6-*E*-, and 2-*E*, 4-*Z*, 6-*E*-4-ethyldeca-2,4,6-triene-1-al. Structural and geometrical elucidation of both alcohols was made by means of spectral evidence as well as by the catalytic hydrogenation leading to the same 4-ethyldecanol. The "b-peak substance" detected in the leaf alcohol reaction products was proved to be identical with 4-ethyldecanol. The treatment of the trienal containing the central *Z*-double bond with sodium under the leaf alcohol reaction condition failed to afford ethyl-propyl-benzyl alcohol, but gave 4-ethyldecanol. This result safely excludes the operation of the previously suspected valence tautomerism (Cope rearrangement) in the leaf alcohol reaction, and accounts for the pathway of the formation of 4-ethyldecanol.

Solvent Effect in a Partial Asymmetric Synthesis. II. S. Inamasu, M. Horiike and Y. Inouye. *Bull. Chem. Soc. Japan,* **42,** 1393 (1969).—Further evidence for the unambiguous solvent polarity dependence of the stereochemistry in the base-catalyzed Michael type condensation was provided by the systems involving (−)-menthyl chloroacetate and methyl acrylate, and (−)-menthyl acrylate and (−)-menthyl chloroacetate with a modification of the work-up. The electrostatic control of the stereoselectivity was interpreted by the same theorem developed in the previous study and some novel features found for the present systems were discussed.

Synthesis of Substituted Aminomalonates by the Reaction of Chloramine with Malonate Carbanions. M. Horiike, J. Oda, Y. Inouye and M. Ohno. *Agr. Biol. Chem.*, **33,** 292 (1969).—Alkyl-, aryl- and aralkyl-substituted diethyl malonate carbanions in ether solution was allowed to react with an excess (2 mole equivalent) of chloramine in the presence of equimolar morpholine for 7 hr. The reaction mixture was worked up as usual and the corresponding substituted aminomalonates were

obtained in 70–95% yields. The first step of this reaction seems to be a radical addition of chloramine to the double bond of the enolate form carbanion. This procedure provides a novel route of synthesis for α-aminoacids through aminomalonates in a simple procedure with easily accessible materials and in satisfactory yields.

Reaction of Aromatic Compounds with Palladium(II) Salts—Acetoxylation of Nucleus, Oxidation of Side Chain and Oxidative Coupling — K. Ichikawa, S. Uemura and T. Okada. *Nippon Kagaku Zasshi*, **90,** 212 (1969), in Japanese. —Palladium(II) nitrate reacted with aromatic compounds in acetic acid to form the products through three kinds of reaction; 1) acetoxylation of aromatic nucleus, 2) oxidation of aromatic side chain, and 3) oxidative coupling of aromatic nucleus. With the addition of water, perchloric acid or iron(III) sulfate *etc.* the nature of the reaction changed from 1) to 3), while the presence of chloride ion retarded all the reactions. With palladium(II) acetate or sulfate, 3) was the main reaction. It is concluded that the acetoxylation proceeds through dehydrogenation-acetoxylation in mono-nuclear π-complex between palladuim salts and aromatics and that the oxidative coupling occurs in bi-nuclear π-complex. Nitration occurred as the side reaction to give, for example, *m*-nitrotoluene which can hardly be expected from normal electrophilic aromatic substitution by nitronium ion. This shows that the nitration in this case proceeds also through palladium-aromatic π-complex.

The Oxidation and Oxidative Coupling of Styrene and α- and β-Methylstyrene with Various Palladium(II) Salts. S. Uemura, T. Okada and K. Ichikawa. *Nippon Kagaku Zasshi,* **89,** 692 (1968), in Japanese. —Reactions of palladium(II) salts with styrene, α- and β-methylstyrene in acetic acid gave various products such as ketones, enol acetate, allyl acetate and butadiene derivatives, depending on the kind of palladium(II) salt. With palladium(II) acetate, α- and β-acetoxystyrene and 1,4-diphenyl-1,3-butadiene from styrene, 2-phenylallyl acetate and 2,5-diphenyl-2,4-hexadiene from α-methylstyrene, and 3-phenylallyl acetate from β-methylstyrene were obtained as the main products, respectively. With palladium(II) nitrate, the main products were ketones. With sulfate, the olefin dimers were mainly formed (1,3-diphenyl-1-butene from styrene and 2,4-diphenyl-4-methyl-2-pentene from α-methylstyrene). In the presence of sodium acetate, the reaction of styrene with palladium(II) acetate or chloride gave enol acetate as the main product and the yields of butadiene derivatives were low.

Reaction of Butadiene with Cupric Chloride in Acetic Acid —Synthesis of Diacetoxybutene— S. Uemura, T. Hiramoto and K. Ichikawa. *Kôgyô Kagaku Zasshi,* **72,** 1096 (1969), in Japanese.—In acetic acid containing sodium acetate, a reaction between butadiene and cupric chloride(II) at 150°C for 5 hr gave a mixture of 3,4-diacetoxy-1-butene and 1,4-diacetoxy-2-butene in 50% yield. The addition of various palladium catalysts to this system increased the yield (58-64%) and the isomer ratio of 1,4- to 3,4-isomer. It was concluded that the 3,4-isomer is converted to the 1,4-isomer by palladium catalysts. A reaction with potassium acetate in place of sodium acetate proceeded similarly, but with lithium acetate the same reaction gave a high boiling polymerized product together with a small amount of diacetoxy-

butenes. Butadiene reacted with palladium acetate(II) also to give a mixture of isomeric diacetoxybutenes.

Liquid Phase Chlorination of Olefins with Cupric Chloride. K. Ichikawa, S. Uemura, T Hiramoto and Y. Takagaki. *Kôgyô Kagaku Zasshi,* **71,** 1657 (1968), in Japanese.—Olefins reacted with cupric chloride to produce dichloroparaffins in various organic solvents (*e.g.* acetic acid, alcohols, acetonitrile, THF and DMF) under reflux. In acetic acid, the reaction was accelerated remarkably by the addition of sodium acetate. The starting materials and the products (described in parentheses) are as follows: Cyclohexene (*trans*-1,2-dichlorocyclohexane), 1-octene (1,2-dichlorooctane), 2-octene (2,3-dichlorooctane), styrene (α-acetoxy-β-chloroethylbenzene, styrene dichloride), ethylene (1,2-dichloroethane) and propylene (1,2-dichloropropane). In the case of butadiene, 3,4-diacetoxy-1-butene and 1,4-diacetoxy-2-butene which are the acetolysis products of the expected dichloro-compounds were obtained. Kinetic experiments showed that this reaction is of first-order with respect to olefin and cupric chloride, respectively, and retarded by cuprous chloride. It is also concluded that the chlorinating agent is not the chlorine produced from cupric chloride but cupric chloride itself. The mechanism of this reaction can be explained by assuming that a complex is formed between the olefin and cupric chloride, and its formation is the rate-determining step. This complex reacts with another cupric chloride molecule to give a dichloroparaffin.

Syntheses of Some Bi-functional Compounds from Dimethyl Terephthalate. S. Shimojo, S. Tanimoto, M. Okano and R. Oda. *Yûki Gôsei Kagaku Kyokai Shi,* **26,** 490 (1968), in Japanese.—Upon treatment of dimethyl terephthalate with methylsulfinylcarbanion in DMSO, a solution of the carbanion of 1,4-bis (methylsulfinyl acetyl) benzene (2) was obtained. When the solution was treated with an aqueous acid, compound (2) underwent Pummerer rearrangement to yield *p*-phenylenediglyoxal bis (methylhemimercaptal) (8), which gave *p*-phenylenediglyoxal (9) on hydrolysis. *p*-Phenylenediglycolic acid (10) was also prepared from (8). Reduction of (2) with zinc dust and acetic acid gave *p*-diacetylbenzene (3) and this was converted to a bisepoxy compound, 1,4-bis (1′,2′-epoxyisopropyl) benzene (7), by the action of a sulfonium methylide. The bis-(Mannich base), 1,4-bis (β-N,N-dimethylaminopropionyl) benzene dihydrochloride (5) derived from (3), formaldehyde, and dimethylamine hydrochloride gave a bispyrazoline by condensation with phenylhydrazine.

Syntheses and Polymerizations of Some β-Oxyalkyl Acrylates. M. Nishi, S. Tanimoto, R. Oda and M. Okano. *Kôbunshi Kagaku,* **25,** 850 (1968), in Japanese. —Several new β-oxyalkyl acrylates (I–VI) were prepared by the trimethylphenylammonium iodide-catalyzed reactions of acrylic acid with some epoxides having branched alkyl, phenyl, cyclohexyl, or N, N-dialkylamino group. Their polymerization was carried out in bulk or in benzen solution using 2,2′-azobisisobutyronitrile as an initiator. In contrast with normal polyacrylates, these polymers showed good solubilities in hydrophilic solvents, which probably arised from the presence of hydroxyl groups. Some polymer reactions on hydroxyl and dialkylamino groups were also attemped. Among them, a cross-linked reaction with TDI gave a hard glass-like resin.

Syntheses of Some Derivatives of Dicyclopropyl Ketone. S. Tanimoto, A. Kita, M. Okano and R. Oda. *Yûki Gôsei Kagaku Kyôkai Shi,* **27,** 444 (1969), in

Japanese.—The syntheses of some new derivatives of dicyclopropylketone are described. Upon treatment with dimethylsulfonium methylide, dicyclopropyl ketone (1) gave 2,2′-dicyclopropyl acetaldehyde (2), which could subsequently be converted into 3,3′-dicyclopropyl propylene oxide (3) by the further attack of the same ylide. Dicyclopropylcarbinol (4) and 2,2′-dicyclopropylethanol (9), prepared from (1) and (2) respectively, were treated with acryloyl chloride and their acrylates thus obtained were bulk polymerized.

1,1-Dicyclopropyl-n-propanol (7) and 2,2′-dicyclopropyl-1-phenethyl alcohol (13), which had been prepared by the Grignard reactions of (1) and (2), were dehydrated over $KHSO_4$ to yield the corresponding olefins (8) and (14), respectively.

An attempted radical polymerization of (8) was unsuccessful. The Ag_2O oxidation of (2) afforded the corresponding acid.

Syntheses and Applications of the Polymers Containing Mannich Base Structure in the Side Chain. S. Tanimoto, J. Horikawa, M. Okano and R. Oda. *Yûki Gôsei Kagaku Kyôkai Shi,* **26,** 680 (1968), in Japanese.—*p*-Vinyl-(β-N,N-dimethylamino)-propiophenone (3), *p*-vinyl-(β-piperidino)-propiophenone (5), β-(*p*-vinylbenzoyl)-propionitrile (4), and 1-phenyl-3-(*p*-vinylphenyl)-pyrazoline (7) were synthesized. (3) and (5) are new styrene derivatives containing Mannich base structure in para positions.

(3) was polymerized in benzene to obtain a polymer with intrinsic viscosity of 0.18 $dl \cdot g^{-1}$ (benzene, 30°C). A small amount of (7) was bulk copolymerized with styrene to obtain a fluorescent polystyrene. Copolymerization of (3) with divinylbenzene and aminomethylation of *p*-vinylacetophenone-divinylbenzene copolymer gave anion-exchange resins with capacities of 3.71 meq/g and 3.64 meq/g, respectively.

Syntheses of Some New Polymers from *p*-Vinylphenol. S. Tanimoto, J. Horikawa, M. Okano and R. Oda. *Yûki Gôsei Kagaku Kyôkai Shi,* **26,** 1102 (1968), in Japanese.—*p*-Vinylphenyl glycidyl ether (1), a new vinyl epoxy monomer, was synthesized in 11.1% yield from *p*-vinylphenol and epichlorohydrin. (*p*-Vinylphenyl)-methane-sulfonate and (*p*-vinylphenyl)-benzenesulfonate were also synthesized, and their polymers prepared.

(1) was bulk-polymerized into a new epoxy resin (3) with intrinsic viscosity of 0.81 $dl \cdot g^{-1}$ (dioxane, 30°C). (1) and (3) appeared to be useful for casting or heat adhesion. By treatment of poly-*p*-vinylphenol with benzenediazonium chloride, a colored polymer containing azo groups was obtained, and with cinnamoyl chloride, a photosensitive polymer was formed.

Reactions of N-Sulfomethylbenzamide Derivatives with Benzamide Derivatives, Phthalimide, Carbazole and Indole. S. Tanimoto, J. Horikawa and R. Oda. *Yûki Gôsei Kagaku Kyôkai Shi,* **27,** 60 (1969), in Japanese. —Four jointed compounds by formaldehyde[N-sulfomethylbenzamide (SMB), *p*-chloro-N-sulfomethylbenzamide (*p*-CSM), N-sulfomethyl-*p*-toluamide (SM-*p*-T) and N-sulfomethyl-*p*-anisamide (SM-*p*-A)] were synthesized, and their transjointing reactions investigated.

Methylenebis-*p*-toluamide(MB-*p*-T), 4,4′-dichloromethylenebisbenzamide(DCM) and diindolylmethane (DIM) were obtained by the reaction between SMB and each one of *p*-toluamide, *p*-chlorobenzamide and indole.

Methylenebisbenzamide (MBB), DCM, MB-*p*-T, methylenebis-*p*-anisamide (MB-*p*-A), *p*-chloro-N-phthalimidomethylbenzamide, N-carbazolylmethyl-*p*-chlorobenzamide and DIM were obtained by the reaction between *p*-CSM and each one of benzamide, *p*-chlorobenzamide, *p*-toluamide, *p*-anisamide, phthalimide, carbazole, and indole.

MBB, DCM, MB-*p*-T, MB-*p*-A, N-phthalimidomethyl-*p*-toluamide, N-carbazolylmethyl-*p*-toluamide and DIM were obtained by the reaction between SM-*p*-T and each one of benzamide, *p*-chlorobenzamide, *p*-toluamide, *p*-anisamide, phthalimide, carbazole and indole.

Similarly, MBB, DCM, MB-*p*-T, MB-*p*-A, N-phthalimidomethyl-*p*-anisamide and DIM were obtained by the reaction between SM-*p*-A and each one of benzamide, *p*-chlorobenzamide, *p*-toluamide, *p*-anisamide, phthalimide and indole, respectively.

Synthesis of Heterocyclic Compounds Using Amidines (Review). S. Tanimoto. *Yûki Gôsei Kagaku Kyôkai Shi,* **27,** 551 (1969), in Japanese.—This paper reviews the synthesis of heterocyclic compounds using amidines.

Syntheses of Polystyrene-Type Reactive Polymers (Review). S. Tanimoto. *Yûki Gôsei Kagaku Kyôkai Shi,* **26,** 849 (1968), in Japanese.—This paper reviews the syntheses and the applications of polystyrene-type reactive polymers.

Polymer Chemistry

Fractionation of Amorphous Polymer with a θ Solvent Column. Nobuo Donkai and Tadao Kotaka. *Kôgyô Kagaku Zasshi*, **71,** 1039 (1968), in Japanese.—Column fractionation experiments have been performed on polystyrene-cyclohexane systems with a Baker-Williams type (temperature-gradient) column to elucidate the basic mechanism of the column fractionation processes. In these experiments, we have employed a procedure for loading the column with polymer samples such that the polystyrene-cyclohexane solutions are directly poured into the column with a prescribed temperature gradient. We have examined whether or not the selective precipitation of the polymer along the column would take place.

For the fractionating elution processes, two procedures have been employed; one is to use cyclohexane with increasing elution temperature, the other is to use mixed solvent (cyclohexane-benzene) with increasing solvent power at a constant temperature gradient. For the former process, we have examined the relation between the elution temperature and the molecular weight of eluted fractions, and the results have been compared with those of Krigbaum. The results are discussed in terms of phase equilibrium relation for polymer-θ solvent systems. For the latter process, the relation between the solvent composition and the molecular weight of the eluted fractions has been examined. A criterion for the choice of adequate solvent-nonsolvent system for the column fractionation, has been discussed.

Sedimentation Transport Method for Determination of Molecular Weight Distributions. T. Kotaka and N. Donkai. *Polymer Sci.: Part A-2,* **6,** 1457 (1968).

—The sedimentation of the system polystyrene-cyclohexane at the Flory temperature has been studied with emphasis on the effects of pressure as well as concentration. The relation between the molecular weight M and the limiting sedimentation coefficient s_0^0, is found to be $s_0^0 = 1.50 \times 10^{-15} M^{1/2}$ (sec.) The concentration dependence parameter k_s has the form, $k_s = k'M^{1/2} = k''s_0^0$, with $k' = 4.5-5.5 \times 10^{-4}$. However, a rather unexpected dependence of k_s on the rotor speed is also found. A procedure is proposed for deducing solute molecular weight distributions from boundary spreading data in sedimentation transport experiments, a so-called "single concentration" method, requiring only one sedimentation run. Application to several polystyrenes (in cyclohexane at 35°C) with narrow, broad, and very broad distributions demonstrates the feasibility of the procedure. Comparisons are made with data from elution chromatography and gel permeation chromatography. The GPC method predicts somewhat broader distributions than those obtained by the other two methods.

Ultracentrifugation Studies on Copolymer Solutions: Application of the Archibald Method for Determination of Molecular Weights. (Note). T. Kotaka, N. Donkai, H. Ohnuma and H. Inagaki. *J. Polymer Sci.: Part A-2*, **6,** 1803 (1963).—An attempt was made to develop a treatment of the Archibald method for solutions of copolymers which are heterogeneous in composition and in molecular weight, and then to demonstrate the applicability of the method for determining the weight-average molecular weight M_w of heterogeneous copolymers. The Archibald apparent molecular weight determined in different solvents can be expressed as a function of the specific refractive-index increment and the buoyancy factor with M_w and two heterogeneity parameters. An experimental test of the theories shows that the Archibald method appears to be applicable to copolymer solutions, and to be especially suited for the analysis of low molecular weight copolymers.

Determination of Compositional Heterogeneity in Copolymers by Thin Layer Chromatography. 1. Preliminary Results for Styrene-Acrylate Copolymers. H. Inagaki, H. Matsuda and F. Kamiyama. *Macromolecules,* **1,** 520 (1968).—The feasibility of determining the compositional heterogeneity of copolymers by thin layer chromatography (tlc) has been demonstrated. Homopolymers and copolymers of styrene (ST) and methyl acrylate (MA) prepared at various monomer feed ratios were used as test samples. Seven solvents, chosed appropriately from the eluotropic series, were used to develop the chromatograms. No intermediate R_f value was observed, since some species remained immobile while others reached the solvent front. Similar, unfavorable results were observed using solvent mixtures. Good separation was achieved by developing in a concentration gradient, using the system carbon tetrachloride-methyl acetate. By this procedure, the composition distribution curve of a high-conversion ST-MA copolymer was determined. The result agreed well with a calculated curve, based on radical copolymerization kinetics. The limitations of the new technique are discussed briefly. Finally, preliminary data are presented indicating that, under suitable conditions, separation of copolymers with respect to differences in steric monomer arrangement is also possible.

Theory of a Rapid Method for Determining Molecular Weights of Giant Molecules. Tadao Kotaka and Robert L. Baldwin. *Biopolymers,* **7,** 87 (1969).—A

new method is proposed for finding molecular weights from the boundary condition of the ultracentrifuge. The method is more rapid than the conventional Archibald method by at least one order of magnitude and should be especially useful for giant molecules with small diffusion coefficients. It employs a present concentration gradient. A theoretical study of the method has been made by obtaining solutions to the Lamm equation analogous to the "mirror image" solution (for early times) and the Fourier expansion solution (for late times) of Mason and Weaver. Numerical examples of theoretical results are given, and the errors are discussed. Centrifugation in a preset linear gradient can also be used to reduce the time needed to reach equilibrium.

Dynamic Viscoelastic Properties of Isothermally Crystallized Polypropylene Fractions. H.-D. Chu, R. Kitamaru and W. Tsuji. *Kôbunshi Kagaku,* **25,** 467 (1968), in Japanese. —The dynamic viscoelastic properties of polypropylene fractions which had been isothermally crystallized from the melts were studied as a function of the crystallization temperature. It was found that the peak position T_α in the dynamic loss-temperature curve which is usually observed in the range of room temperature shifts to a lower temperature with the increase of the crystallization temperature.

From the results of the measurements for the samples which were crystallized at 110–155°C for a very long period of time, it was concluded that the amorphous chains coexisting with the very stable crystalline phase are in a sufficiently relaxed state: the micro-brownian mobility of the amorphous chain segments in the samples crystallized at the high temperature is not so strongly restricted by crystallites as in the case of lower crystallization temperature (110°C), even though the crystallinity of the sample crystallized at high temperature is higher than that of the sample crystallized at low temperature.

It was also found that T_α shifts to a lower temperature as the molecular weight of the sample decreases. This result can be well understood by the concept that the concentration of the chain end groups in the amorphous phase inevitably increases as the molecular weight decreases, since the end groups would be removed from the crystalline phase to the amorphous phase during the isothermal crystallization at the high temperature close to the melting point.

The Oriented Crystallization of Polymers. R. Kitamaru. *"The Formation of Fiber and The Development of Fiber Structure," The special issue of "Kagaku,"* **No. 39,** 145 (1969), in Japanese.—The crystallization kinetics of polymers is briefly reviewed. The kinetics of a polyethylene gel, isothermally crystallized from the oriented melt, is discussed in terms of the chain conformation.

Brownian Motion of Lattice-Model Polymer Chains. Kazuyoshi Iwata and Michio Kurata. *J. Chem. Phys.,* **50,** 4008 (1969).—The dynamical behavior of lattice-model polymer chains is studied by assuming the Markoff nature of the motion of chain elements. In accord with the Monte Calro calculations of Verdier, the autocorrelation function obtained for the square of the end-to-end distance of a simple-cubic-lattice-model chain is in close agreement with that for a spring-bead-model

chain. The diffusion equation for the lattice-model chain is also exactly similar to that for the spring-bead-model chain. The diffusion constant for a lattice element is found to be $pl^2/3$ and the equivalent spring constant to be $3kT/l^2$. Here, l is the lattice constant, p is the probability that a given chain element moves to its adjacent lattice points in unit time, and kT has the usual meaning.

Determination of Molecular Weight and Second Virial Coefficient of Polydisperse Nonideal Polymer Solutions by the Sedimentation Equilibrium Method. Hiroyasu Utiyama, Nobuo Tagata, and Michio Kurata. *J. Phys. Chem.*, **73,** 1448 (1969).—Sedimentation equilibrium experiments have been carried out in order to establish the experimental procedure and the method to determine the weight-average molecular weight and the light-scattering second virial coefficient on polydisperse nonideal polymer solutions. The experimental condition was chosen so that the most accurate results may be obtained under the requirement that the equilibrium is established within 20 hr with a sample of molecular weight of several millions. Two samples of monodisperse polystyrene S_A (mol wt $= 1.97 \times 10^6$) and S_B (mol wt $= 0.162 \times 10^6$) and four polydisperse samples made up of S_A and S_B were examined in 2-butanone at 25.0°. With the Rayleigh interference optical system and the column height of 0.15 cm, the weight-average molecular weight is obtained correct to within $\pm 2\%$ irrespective of the degree of polydispersity. The accuracy of the determination of the light-scattering second virial coefficient, on the other hand, depends very much on the detail of the molecular weight distribution. If the molecular weight of the minor component is very large compared with that of the major component, the experimental error amounts to as large as 10%. The uncertainty becomes greater as the second virial coefficient increases. It has been found for evaluating the apparent molecular weight in the limit that λ approaches zero, the plot of M_{app}^{-1} *vs.* λ^2 is the most appropriate. It has also been concluded that the weight-average molecular weight and the light-scattering second virial coefficient for polymers with unknown molecular weight distribution should be evaluated from the plot of $\lim_{\lambda \to 0} M_{app}^{-1}$ *vs.* c_0, instead of the plot of $\lim_{\lambda \to 0} M_{app}$ *vs.* c_0.

Biochemisty

The Effects of Pressure on Actomyosin Systems. Takamitsu Ikkai and Tatsuo Ooi. *Biochemistry,* **8,** 2615 (1969).—The interactions of actin with myosin, heavy meromyosin, and subfragment 1 were investigated under pressure from 1 atm up to 4000 Kg/cm^2. Summarizing the results, the pressure effects on actomyosin systems are accounted for in terms of depolymerization or dissociation of protein components, and adenosine triphosphate plays an important role in interactions of actin and heavy meromyosin.

Length of RNA Transcribed on the Replicative Form DNA of Coliphage fd. T. Okamoto, M. Sugiura and M. Takanami. *J. Mol. Biol.*, **45,** 101 (1969).—The length of RNA synthesized on the doubly-closed replicative form DNA of coliphage fd was determined based on the fact that the RNA chains were initiated predominantly

with purine nucleotides. It was found that three species of RNA of which the molecular weights were 4.5×10^5, 6.2×10^5 and 1.3×10^6 daltons were synthesized under the direction of the replicative form DNA. The RNA-synthesizing system contained no detectable RNase and the sizes of the RNA's synthesized were markedly different depending on the initial nucleotides. It was suggested that the replicative form DNA provided specific sites for the termination of RNA synthesis in addition to specific initiation sites.

Starting Nucleotide Sequences of RNA synthesized on the Replicative Form DNA of Coliphage fd. M. Sugiura, T. Okamoto and M. Takanami. *J. Mol. Biol.*, **43**, 299 (1969).—The replicative form DNA, with no single-strand break, was purified from *Escherichia coli* cells infected with a filamentous coliphage fd, and the starting nucleotide sequences of RNA formed by *E. coli* RNA-polymerase under the direction of the replicative form DNA as template were analysed. It was found that at least three species of RNA starting with the following sequences were synthesized under the direction of the replicative form DNA of phage fd:

$$_{ppp}A_pU_pG_p\ldots,\quad _{ppp}G_pU_pA_p\ldots,\quad _{ppp}G_pU_pU_p\ldots.$$

Two of the sequences are the proposed initiation codons for protein synthesis.

Purification of L-Lysine-α-Ketoglutarate Transaminase and Its Properties. Kenji Soda and Haruo Misono. *Amino Acid and Nucleic Acid,* **18,** 83 (1968), in Japanese.—L-Lysine-α-ketoglutarate transaminase was purified and crystallized from the cell-free extract of *Achromobacter liquidum*. The purified enzyme is homogeneous by the criteria of ultracentrifugation and electrophoresis. The molecular weight and $S^0_{20,w}$ are 116,000 and 6.37 S, respectively. Two moles of pyridoxal 5'-phosphate are bound to 1 mole of holoenzyme. The enzyme exhibits absorption maxiam at 340 mμ and 415 mμ in addition to 280 mμ, and no appreciable spectral change was observed on varying pH.

Treatment of the enzyme with L-lysine in the presence of a high concentration of phosphate gave an inactive form of the enzyme which could be reactivated with pyridoxal 5'-phosphate and pyridoxamine 5'-phosphate. This inactive form of the enzyme does not exhibit an absorption maximum at 415 mμ, but exhibits one at 340 mμ, and contains 1 mole of pyridoxal 5'-phosphate per mole of the enzyme.

The enzyme catalyzes also transfer of the terminal amino group of L-ornithine to α-ketoglutarate.

L-Lysine-α-Ketoglutarate Aminotransferase. 1. Identification of a Product, Δ^1-Piperideine-6-carboxylic Acid. Kenji Soda, Haruo Misono, and Tatsuo Yamamoto. *Biochemistry,* **7,** 4102 (1968).—The product derived from L-lysine was isolated from the L-lysine-α-ketoglutarate aminotransferase system of *Flavobacterium fuscum* and its properties were studied. Radioactivity from DL-[1-^{14}C] lysine was incorporated exclusively into a product which reacted with *o*-aminobenzaldehyde. Chromatographic and electrophoretic studies, characterization of the bisulfite and *o*-aminobenzaldehyde adducts and the condensation product, and comparison with authentic Δ^1-piperideine-2-carboxylic acid offer evidence that the product is Δ^1-

piperideine-6-carboxylic acid. In this aminotransferase reaction, ϵ-amino group of L-lysine is transferred to α-ketoglutarate to yield glutamate and α-aminoadipate-δ-semialdehyde which is immediately converted into the intramolecularly dehydrated form, Δ^1-piperideine-6-carboxylic acid.

L-Lysine-α-Ketoglutarate Aminotransferase. II. Purification, Crystallization, and Properties. Kenji Soda and Haruo Misono. *Biochemistry*, **7**, 4110 (1968).—The preparation of crystalline L-lysine-α-ketoglutarate aminotransferase from *Achromobacter liquidum* is described. The enzyme is homogeneous by the criteria of ultracentrifugation, free-boundary electrophoresis, and disc gel electrophoresis. The molecular weight is 116,000, and 2 moles of pyridoxal 5'-phosphate are bound per mole of holoenzyme. The enzyme exhibits absorption maxima at 415 and 340 mμ. No appreciable spectral change was observed on varying pH. Addition of an amino donor to the enzyme produced a decrease in the absorbance at 415 mμ and an increase in that in the 340 mμ-region with concomitant shift of the maximum from 340 to 330 mμ. The spectrum of the enzyme was not influenced by addition of α-ketoglutarate. Incubation of the enzyme with L-lysine in the presence of a high concentration of phosphate gave an inactive form of the enzyme (semiapoenzyme) which could be reactivated with pyridoxal 5'-phosphate. The absorption spectrum of semiapoenzyme does not have an abosorption maximum at 415 mμ, but does have one at 340 mμ. This inactive form of enzyme contains 1 mole of pyridoxal 5'-phosphate. L-lysine-α-ketoglutarate aminotransferase exhibits optimal activity at pH 8.3-8.5; it is stable over the pH range 6.0-7.5. It catalyzes transfer of the terminal amino groups of L-lysine and L-ornithine to α-ketoglutarate which is the exclusive amino acceptor. The following Michaelis constants were determined: L-lysine (2.8×10^{-3} M), α-ketoglutarate (5.0×10^{-4} M), and pyridoxal 5'-phosphate (3.57×10^{-7} M).

Microdetermination of D-Amino Acids and D-Amino Acid Oxidase Activity with 3-Methyl-2-benzothiazolone hydrazone Hydrochloride. Kenji Soda. *Analytical Biochemistry*, **25**, 228 (1968).—A simple and rapid technique for the determination of the D-amino acids which are oxidized by D-amino acid oxidase has been presented. This method involves an oxidation of D-amino acids with D-amino acid oxidase in the presence of catalase, and the spectrophotometric determination of the resultant α-keto acids with MBTH. The additions of L-amino acids have no influence on the quantitative estimation of D-amino acids. The method is suitable for the assay of D-amino acids in the presence of the L isomers, and is also applicable for the determination of D-amino acid oxidase activity.

Pyridoxal Phosphate Enzymes. Kenji Soda. *Kagaku to Seibutsu*, **7**, 28 (1969), in Japanese.—The structures and physiological functions of vitamin B_6 compounds were described in order to throw light on understanding their role as the coenzyme in pyridoxal phosphate enzymes. The review on the mechanisms of the model and enzymatic systems of pyridoxal phosphate enzymes, *e.g.*, aminotransferase, was presented.

Amino Acid Racemase—The diversity of substrate and cofactor. Kenji Soda. *Kagaku to Seibutsu*, **6**, 531 (1969), in Japanese.—The various mechanisms of

enzymatic racemization of amino acids were illustrated and the history of investigation on the racemases was described. The recent advances in enzymology of amino acid racemase, especially studies on the diversity of substrate and cofactor, were reviewed.

Crystalline Lysine Decarboxylase. Kenji Soda and Mitsuaki Moriguchi. *Biochem. Biophys. Res. Commun.*, **34,** 34 (1969).—Lysine decarboxylase (L-lysine carboxylase, E.C. 4.1.1.18) was isolated, purified by means of heat treatment, ammonium sulfate fractionation, DEAE-Sephadex chromatography and Sepharose 4B chromatography, and crystallized from the sonic extract of *Bacterium cadaveris* IFO 3731. The crystals obtained take the form of fine rods with a yellow color. The crystalline enzyme is homogeneous according to the criterion of ultracentrifugation. An $S^{0}_{20,w}$ value of 21.1 S was calculated from the sedimentation rate for zero protein concentration. The molecular weight of the enzyme is 1,000,000±50,000, assuming a partial specific volum of 0.74. The spectrum of the enzyme exhibited two absorption maxima at 280 and 425 mμ; these give an absorption ratio of 12 : 1. No appreciable spectral shifts occurs when pH is varied. The enzyme has an optimum reactivity at 5.8, and the K_m value is 3.7×10^{-4} M. The decarboxylase contains 10 moles of pyridoxal 5'-phosphate per mole of enzyme, when examined by the phenylhydrazine method and the cyanohydrin procedure.

Enzymatic Racemization of Leucine and α-Aminobutyrate. Part II. Distribution of Amino Acid Racemase Activity, Identification of the Organism and New Assay Method of Enzyme. Kenji Soda, Takaharu Osumi, Takamitsu Yorifuji and Koichi Ogata. *Agr. Biol. Chem.*, **33,** 424 (1969).—The distribution of amino acid racemase activities was investigated in the cell-free extracts of various strains of bacteria. Alanine racemase activity was exclusively found in all the strains tested. However, the cell-free extract of Strain 25-3, which has been identified as *Pseudomonas striata,* possessed the high activity catalyzing the racemization of alanine, α-aminobutyrate, leucine and methionine. The new and sensitive assay method of amino acid racemase with D-amino acid oxidase and 3-methyl-2-benzothiazolone hydrazone hydrochloride was established.

Enzymatic Racemization of Leucine and α-Aminobutyrate. Part III. Properties of partially purified Racemase. Takaharu Osumi, Tatsuo Yamamoto and Kenji Soda. *Agr. Biol. Chem.*, **33,** 430 (1969).—A new amino acid racemase catalyzing the conversion of either D or L enantiomorph of leucine and α-aminobutyrate to the racemates, was partially purified from the cell-free extract of *Pseudomonas striata.* Both the racemase reactions are suggested to be catalyzed by a single enzyme because of the constant ratio between the activities during the purification, and of their very resemble behavior to pH, temperature and heating the enzyme. Pyridoxal phosphate functions as the coenzyme for this racemase.

Crystalline Arginine Racemase. Takamitsu Yorifuji, Koichi Ogata, and Kenji Soda. *Biochem. Biophys. Res. Commun.*, **34,** 760 (1969).—Arginine racemase has been purified from the extract of *Pseudomonas graveolens* approximately 2,300-fold by a procedure including column chromatography on DEAE-cellulose, DEAE-Sephadex

and Sephadex G-150. The purified enzyme was crystallized. The crystalline enzyme is homogeneous upon analysis by ultracentrifugation, and its molecular weight is 167,000. The enzyme exhibits absorption maxima at 280 mμ and 420 mμ, and contains firmly bound pyridoxal 5'-phosphate.

Bacterial N-Acetylation of an L-Lysine Antagonist, S-(β-Aminoethyl)-L-cysteins. Kenji Soda, Hidehiko Tanaka, and Tatsuo Yamamoto. *Arch. Biochem. Biophys.*, **130,** 610 (1969).—*Aerobacter aerogenes* was found capable of growing well in the medium containing *S*-(β-aminoethl)-L-cysteine, a metabolic antagonist of L-lysine, as a sole nitrogen source. The metabolic product has been isolated, purified, and identified as *S*-(β-*N*-acetyl-aminoethyl)-L-cysteine by comparison with the synthetic compound on the basis of studies by paper electrophoresis, paper and ion-exchange chromatographies, nuclear magnetic resonance spectroscopy, infrared spectrophotometry, x-ray diffraction, absorption spectrophotometry of ninhydrin color, elemental analysis, optical rotation, and reaction with L-lysine decarboxylase. The metabolic function of this *N*-acetylation is discussed.

Transamination of *S*-(β-Aminoethyl)-L-cysteine by L-Lysine : α-Ketoglutarate Aminotransferase. Kenji Soda, Haruo Misono, and Tatsuo Yamamoto. *Biochim. Biophys. Acta,* **177,** 364 (1969). —The crystalline L-lysine-α-ketoglutarate aminotransferase was found capable of catalyzing the transfer of the terminal amino group from *S*-(β-aminoethyl)-L-cysteine, a sulfur analog of L-lysine, to α-ketoglutarate at a reaction rate 16% of that for L-lysine. The product from *S*-(β-aminoethyl)-L-cysteine was isolated and its properties were investigated by comparison with that of Δ^1-piperideine-6-carboxylate, which is a transamination product from L-lysine. Paper electrophoretic and chromatographic studies, characterization of the bisulfite adduct and the colored reaction product with *o*-aminobenzaldehyde offer good evidence that the product is 4-thia-Δ^1-piperideine-6-carboxylate which is spontaneously derived from *S*-(formylmethyl)-L-cysteine, a direct product from the amino donor, as follows.

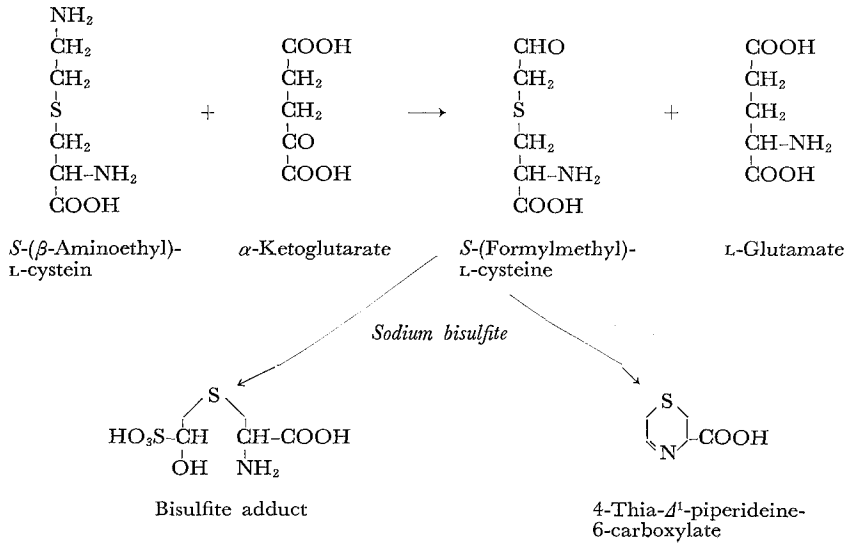

Crystalline Amino Acid Racemase with Low Substrate Specificity. Kenji Soda and Takaharu Osumi. *Biochem. Biophys. Res. Commun.*, **35,** 363 (1969).—The preparation of crystalline amino acid racemase with low substrate specificity from *Pseudomonas striata* is described. The enzyme is homogeneous by the criteria of ultracentrifugation and disc gel electrophoresis. The molecular weight is 110,000. The enzyme exhibits absorption maxima at 280 and 420 mμ, and requires pyridoxal 5'-phosphate for the maximal activity. Leucine, α-aminobutyric acid, alanine, norvaline, norleucine, arginine, methionine, lysine, and ethionine are racemized by this enzyme in the order of increasing the reactivity.